





A versatile microbial platform as a tunable whole-cell chemical sensor

Received: 8 May 2024

Accepted: 17 September 2024

Published online: 27 September 2024

 Check for updates

Javier M. Hernández-Sancho¹, Arnaud Boudigou¹, Maria V. G. Alván-Vargas¹, Dekel Freund², Jenny Arnling Bååth³, Peter Westh³, Kenneth Jensen⁴, Lianet Noda-García², Daniel C. Volke¹  & Pablo I. Nikel¹  

Biosensors are used to detect and quantify chemicals produced in industrial microbiology with high specificity, sensitivity, and portability. Most biosensors, however, are limited by the need for transcription factors engineered to recognize specific molecules. In this study, we overcome the limitations typically associated with traditional biosensors by engineering *Pseudomonas putida* for whole-cell sensing of a variety of chemicals. Our approach integrates fluorescent reporters with synthetic auxotrophies within central metabolism that can be complemented by target analytes in growth-coupled setups. This platform enables the detection of a wide array of structurally diverse chemicals under various conditions, including co-cultures of producer cell factories and sensor strains. We also demonstrate the applicability of this versatile biosensor platform for monitoring complex biochemical processes, including plastic degradation by either purified hydrolytic enzymes or engineered bacteria. This microbial system provides a rapid, sensitive, and readily adaptable tool for monitoring cell factory performance and for environmental analyzers.

Industrial microbiology and metabolic engineering use the Design-Build-Test-Learn cycle (DBTLc) to endow cell factories with specific phenotypes suitable for production processes^{1–3}. The rapid progress in genetic^{4,5} and protein engineering^{6,7}, along with advances in automation protocols⁸, have accelerated the design and build phases of the DBTLc. However, the test phase remains a major bottleneck owing to its substantial time and labor demands. The intricacies inherent to living organisms restrict the user's ability to estimate the outcome of engineering efforts (for example, a production phenotype) when modifying multiple biological components^{9–11}, such as coding sequences, promoters, and ribosome binding sites (RBSs). An engineered system's performance is commonly tested by determining product concentrations. Classical screening methods, however, remain relatively costly and time-consuming¹², compounded by the absence of universal high-throughput techniques that can be applied to the detection of structurally unrelated chemicals¹³.

Biosensors have emerged as an alternative to facilitate screening and selection of efficient cell factories, with multiple application examples^{14–17}. These analytical devices transform biological reactions into quantifiable signals, with reactions executed by entire cells (whole-cell biosensors, WCBs) or by their individual components, such as enzymes, transcription factors (TFs), and aptamers^{18–22}. Detection of chemicals by WCBs is often tied to the expression of fluorescent reporter genes in transducer-based systems amenable to high-throughput detection methods, such as flow cytometry. In these cases, analyte recognition occurs through (i) allosteric TFs, which control reporter expression through analyte-promoter recognition¹⁸; (ii) riboswitches, which trigger gene expression through structural alterations upon ligand binding²³; (iii) two-component systems, which rely on kinase activation by analytes to initiate gene expression²⁴; or (iv) fluorescent and color-based sensors, which alter their output upon interacting with the analyte²⁵. Each of these approaches must be

¹The Novo Nordisk Foundation Center for Biosustainability, Technical University of Denmark, Kongens Lyngby, Denmark. ²Institute of Environmental Sciences, Robert H. Smith Faculty of Agriculture, Food and Environment, Hebrew University of Jerusalem, Rehovot, Israel. ³Department of Biotechnology and Biomedicine Interfacial Enzymology, Technical University of Denmark, Kongens Lyngby, Denmark. ⁴Novonesis A/S, Kongens Lyngby, Denmark.

 e-mail: chdavo@biosustain.dtu.dk; pabnik@biosustain.dtu.dk

assessed for each analyte on a case-by-case basis, as there is no one-fits-all technique²⁶. Analyte-binding sites are difficult to engineer and thus limit the scope of detectable chemicals, since analyte-protein interactions are very selective.

Growth-coupled WCBs offer several advantages over transducer-based systems. In this case, metabolite detection is linked to cell viability in growth-coupled experiments that correlate the presence of the analyte of interest with biomass formation or the expression of antibiotic resistance markers^{27–31}. The engineering of growth-coupled WCBs is facilitated by the diverse repertoire of control elements that bacteria have evolved for detecting and responding to a broad spectrum of chemicals in the environment^{32–34}. Catabolism and assimilation routes^{35–37} can be harnessed for chemical sensing, circumventing the need for specific recognition elements, and enabling the detection of a broad range of analytes. By implementing synthetic auxotrophies in these pathways, a growth deficiency is created that can be restored only by the metabolite to be tested^{38–40}, thereby coupling microbial growth to analyte detection.

The field of growth-coupled WCB engineering is promising and holds strong potential for further development to accelerate the DBTLC. Growth-coupled approaches based on synthetic auxotrophies, however, have been largely restricted to the detection of endogenous metabolites^{41–44}. While TF-based biosensors have been implemented to detect multiple analytes with high sensitivity, including heavy metals⁴⁵ and aromatic hydrocarbons⁴⁶, additional strategies are required for the detection of other complex chemical substrates and xenobiotics. Examples of such analytes include synthetic pharmaceuticals (for instance, fluoxetine) and toxic building blocks (such as bisphenol A), which can only be detected by expensive HPLC, GC-MS, or LC-MS-based analytics^{47,48}. Signal detection in industrial and environmental contexts is particularly difficult due to interference stemming from the growth of other organisms or non-biological turbidity in the medium.

In this work, we present a versatile WCB platform to detect and quantify a variety of chemicals. We chose the non-pathogenic soil bacterium *Pseudomonas putida*, known for its diverse and adaptable metabolism⁴⁹, as the starting point for WCB engineering. The ability of *P. putida* to use structurally diverse molecules as substrates^{50–52} facilitated the rewiring of carbon metabolism to create synthetic auxotrophies. A fluorescent output, proportional to the cell density, was also integrated to broaden the limit of detection in growth-coupled setups. The resulting WCB strains were used to sense and quantify structurally diverse chemicals across a wide concentration scale, using microbial growth and fluorescence as primary outputs. We were able to detect value-added industrial products, including D-lactate and aromatic compounds, and monitor environmental processes, such as the enzymatic degradation of polyethylene terephthalate (PET). We also adapted our system to fit different screening formats (Fig. 1A), including analyzing culture supernatants, monitoring enzymatic activities in vitro, and tracking plastic degradation in vivo within a bacterial co-culture system. Our microbial WCB platform offers a robust and adaptable solution for detecting a broad range of chemicals and is suitable for multiple experimental setups, including high-throughput screening.

Results

Rewiring sugar catabolism in *P. putida* to establish a platform WCB strain

P. putida uses a broad spectrum of structurally diverse molecules as carbon substrates, including aromatic compounds, volatile fatty acids, sugars, and organic acids⁵¹. The diversity of biochemical pathways involved in the assimilation of these substrates offers attractive opportunities to create synthetic auxotrophies for growth-coupled selection³⁵, and a wide synthetic biology toolbox is available to facilitate metabolic rewiring in this bacterium^{53–57}. *P. putida* can be engineered to render an analyte of interest as an essential precursor for

bacterial growth, such that biomass formation correlates with the availability of the essential molecule. Furthermore, we reasoned that fluorescent reporters can be combined with synthetic auxotrophies to facilitate analyte detection within the low concentration range.

We applied a combinatorial approach, without the use of specific analyte-recognizing TFs common in transducer-based systems. We aimed to generate a system with the ability to (i) easily detect biomass formation with a fluorescence output over a broad range of cultivation setups, from single-cell growth to high-cell-density cultures; (ii) readily sense extracellular molecules, allowing for separate detection and production in microbial co-cultures; (iii) adjust the operational range through the strength of the growth-coupling dependency, by calibrating the concentration of a given metabolite needed to generate biomass; and (iv) detect several compounds or even analyte families for different applications with a single WCB design.

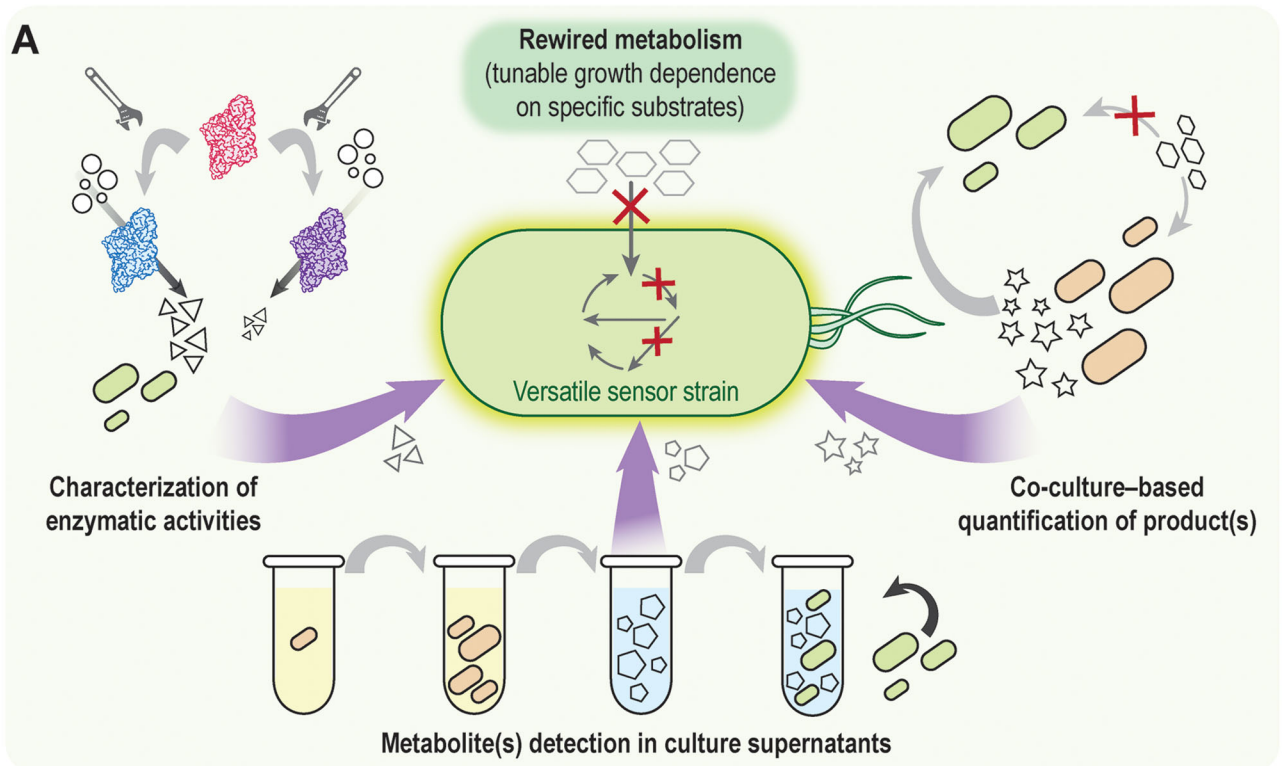
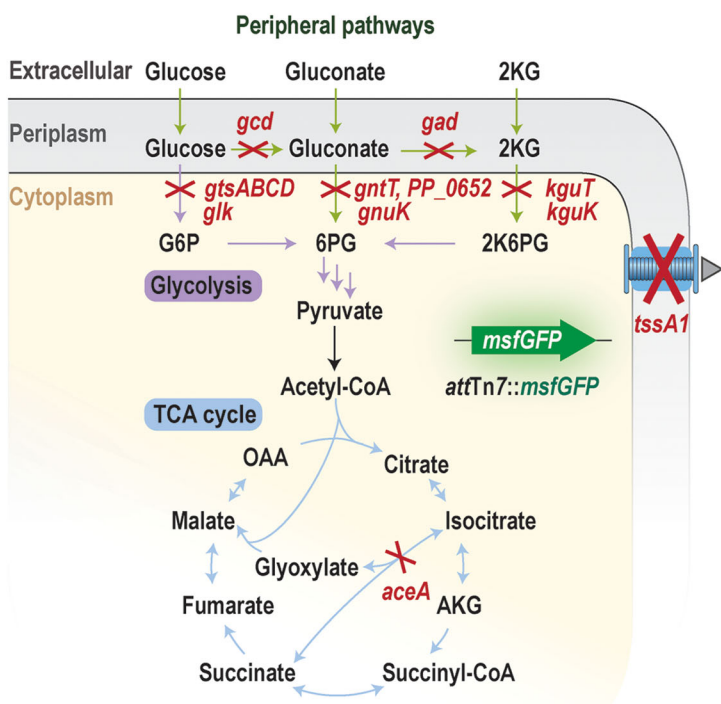
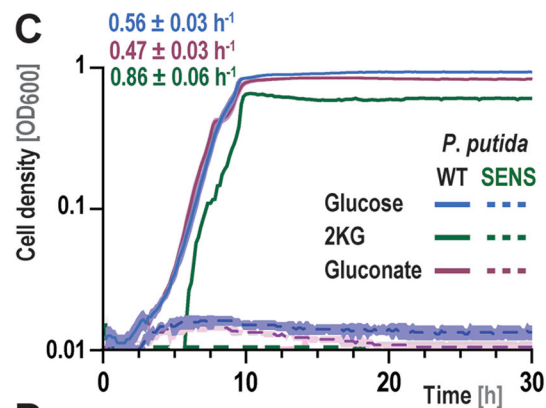
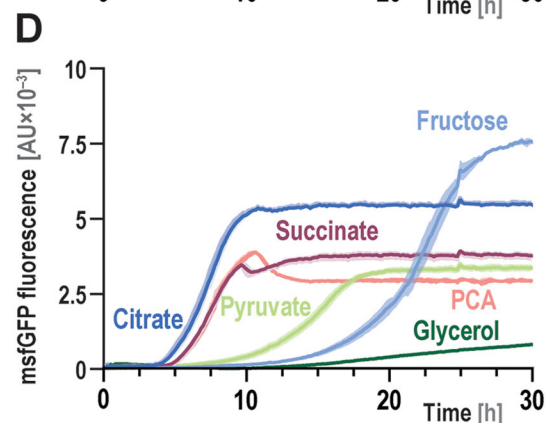
Building on these concepts, we first engineered a *P. putida* strain designed as a sensor suitable for different applications (Fig. 1A). Since most bioprocesses for chemical production use sugar feedstocks, such as products derived from lignocellulosic substrates, glucose assimilation was blocked as a requisite for growth-coupled detection of chemicals. Using a series of in-frame gene knockouts (Supplementary Table 1 and 2), we disrupted the uptake, oxidation, and downstream catabolism of glucose^{58,59}. These 10 gene deletions were expected to deactivate the utilization of all three *P. putida* hexose substrates (glucose, gluconate, and 2-ketogluconate; Fig. 1B). Additionally, an *msfGFP* reporter gene, under transcriptional control of the constitutive P_{14g} promoter⁶⁰, was integrated into the genome via Tn7-mediated chromosomal insertion (Fig. 1B), allowing for monitoring growth through fluorescence. We called this first-generation strain *P. putida* SENS, the starting point for a family of WCB strains designed for chemical sensing (Supplementary Fig. 1 and Table 1).

We next phenotypically characterized this strain in batch cultivations using different carbon substrates in de Bont minimal (DBM) medium. The parental strain (*P. putida* KT2440) could grow on all three hexose substrates with doubling times between 0.8 and 1.5 h, whereas *P. putida* SENS was not able to metabolize any of these sugars even upon prolonged incubation (Fig. 1C). The use of alternative carbon sources was unrestricted: *P. putida* SENS could metabolize glycerol; other carbohydrates (fructose); organic acids feeding either the tricarboxylic acid (TCA) cycle (succinate and citrate) or the lower glycolysis pathway (pyruvate; Fig. 1D); and an aromatic substrate (protocatechuate; PCA). We verified a linear relationship between the fluorescence signal and biomass concentration during the exponential growth phase with all substrates (Supplementary Fig. 2), indicating that *msfGFP* fluorescence can be adopted as a proxy of bacterial growth. Based on these results, we tested *P. putida* SENS for chemical detection in a variety of processes.

Sensing protocatechuate production in *Pseudomonas* co-cultures

We next tested whether we could use the SENS strain to detect and quantify an extracellular molecule, PCA, in microbial co-cultures. PCA is a valuable precursor for pharmaceuticals, flavors, and fragrances, and biotechnological production of this aromatic compound has gained interest in reducing our dependence on petrochemistry⁶¹. Because the SENS strain is unable to use glucose but grew efficiently on PCA as the sole carbon source, we paired it with a *P. putida* producer strain that grows on glucose and synthesizes PCA from sugars (*P. putida* PCA). We have engineered this producer strain to overexpress genes encoding rate-limiting enzymes in PCA biosynthesis, and also is also engineered to suppress feedback inhibition, PCA degradation, and the rerouting of precursors away from competing pathways⁵⁴.

To verify that the growth and fluorescence of *P. putida* SENS can be used as a proxy for sensing PCA, we incubated this strain in the presence of varying concentrations of PCA (0.075 to 75 mM, Fig. 2A).

**B****C****D**

While growth rates did not substantially vary with the PCA concentration up to 50 mM, the end-point normalized fluorescence values (derived from measurements of the msfGFP fluorescence and the optical density at 600 nm, OD₆₀₀) showed a linear correlation with the initial PCA concentration up to 50 mM ($R^2 = 0.98$; Fig. 2B), even at the lowest concentrations tested (0.075, 0.15, and 0.3 mM; Fig. 2B, inset). At high substrate concentrations, microbial growth on aromatic

substrates could be limited by oxygen transfer, especially in microtiter well plates. At 75 mM PCA, the cell density remained low even after 40 h of cultivation, probably due to substrate toxicity⁶².

Motivated by these results, we cultured *P. putida* SENS and the *P. putida* PCA producer strain strains in DBM medium supplemented with 20 mM glucose in different formats (Fig. 2C). Growth and msfGFP fluorescence were continuously recorded in a microtiter plate reader.

Fig. 1 | Engineering *P. putida* as a broadly applicable sensor for structurally diverse chemicals. **A** General concept underlying whole-cell chemical detection by sensor strains. Rewiring the metabolism of *P. putida* enables selective assimilation of specific analytes (gray symbols), allowing for growth-dependent detection. The applications in this study (testing the efficiency of in vitro enzymatic activities, detecting industrially relevant metabolites produced by cell factories, and characterizing plastic breakdown by engineered bacteria in a co-culture system) are indicated in the diagram. **B** Metabolic rewiring of *P. putida* KT2440 to develop the first-generation SENS strain. Assimilation of glucose and its oxidized derivatives, gluconate and 2-ketogluconate (2KG), was blocked by eliminating genes encoding sugar transporters (*gtsABCD*, glucose transporter; *gntT* and *PP_0652*, gluconate transporters; and *kgtK*, 2KG transporter), sugar kinases (*glk*, glucose kinase; *gnuK*, gluconate kinase; and *kguK*, 2KG kinase), and specific dehydrogenases (*gcd*, glucose dehydrogenase; and *gad*, gluconate dehydrogenase). Isocitrate lyase (*aceA*)

and a key gene of the type VI secretion system (*tssA1*) were deleted in derivatives of the first-generation SENS strain for specific applications. The reporter module comprises a constitutively expressed *msfGFP* gene, inserted in the genome at the Tn7 attachment site (*attTn7*). Abbreviations: *TCA cycle*; tricarboxylic acid cycle; *G6P*, glucose-6-phosphate; *6PG*, 6-phosphogluconate; *2K6PG*, 2-keto-6-phosphogluconate; *OAA*, oxaloacetate; *AKG*, α -ketoglutarate; and *CoA*, coenzyme A. **C** Growth profile of wild-type (WT) *P. putida* KT2440 and the sensor SENS strain on different sugars. Both strains were incubated in de Bont minimal medium supplemented with either glucose, gluconate, or 2KG; cell density was estimated as the optical density at 600 nm (OD_{600}). Specific growth rates are indicated. **D** Fluorescence profile of strain SENS grown on different carbon sources supplemented at 10 mM. Cultures were prepared as indicated for panel (C); abbreviations: *PCA*, protocatechuate; AU, arbitrary units. In all cases, results represent average values \pm standard deviations from three independent experiments.

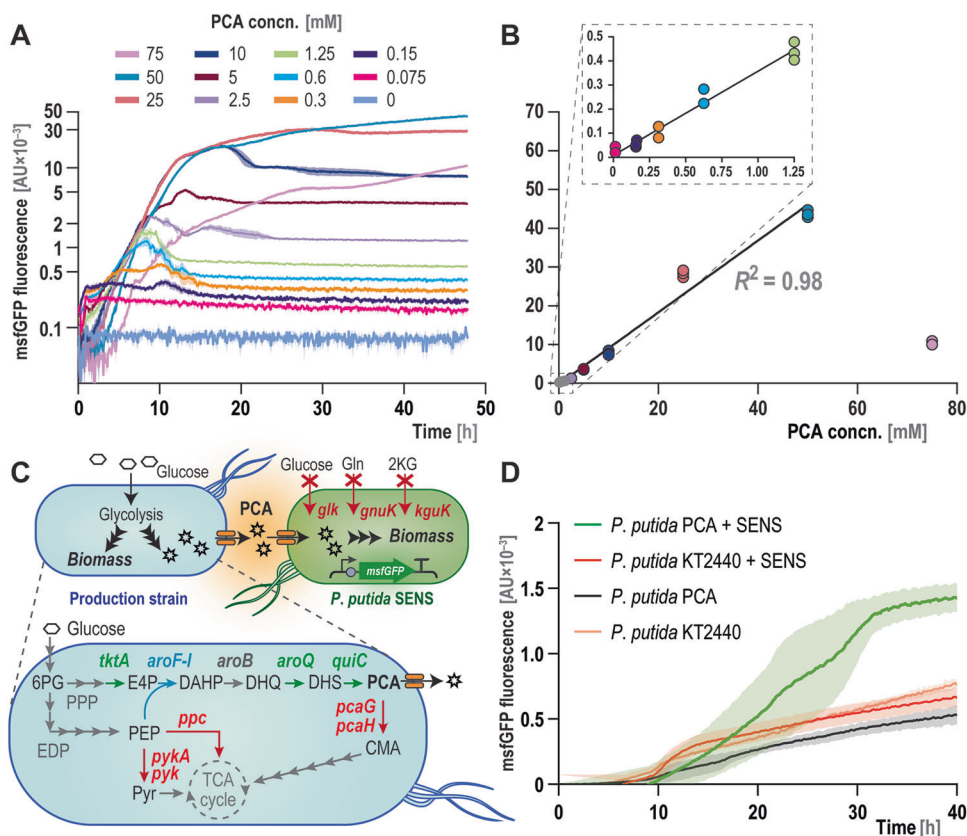


Fig. 2 | Sensing protocatechuate in a bacterial co-culture. **A** *P. putida* SENS was grown in DBM minimal medium with varying concentrations (conc.) of protocatechuate (PCA). The *msfGFP* fluorescence was continuously monitored during growth and is plotted in semi-logarithmic scale. Abbreviation: AU, arbitrary units. **B** Correlation between final fluorescence signals and supplemented PCA. The inset shows the regression at low PCA concerns. (50 μ M to 1 mM, $R^2 = 0.97$). **C** Principle of the co-culture for detection of PCA produced by cell factories. **A** *P. putida* strain engineered for PCA biosynthesis (*P. putida* PCA) consumes glucose and produces PCA, while the sensor strain is unable to utilize sugars, but grows on the PCA secreted by the producer strain. *P. putida* PCA has several competing pathways knocked out (*ppc*, *pyk*, *pykA*, *pcaG*, and *pcaH*), rate-limiting enzymes are over-produced (TkTA, AroQ, and QuiC), and the *aroF-I* gene was modified to remove

feedback inhibition. Abbreviations: *6PG*, 6-phosphogluconate; *PEP*, phosphoenolpyruvate; *Pyr*, pyruvate; *E4P*, erythrose 4-phosphate; *DAHP*, 3-deoxy-D-arabinoheptulosonate 7-phosphate; *DHQ*, 3-dehydroquininate; *DHS*, 3-dehydroshikimate; *CMA*, β -carboxy-*cis,cis*-muconate; *EDP*, Entner-Doudoroff pathway; *PPP*, pentose phosphate pathway; *TCA cycle*, tricarboxylic acid cycle. **D** *msfGFP* fluorescence in co-cultures of the producer strain (*P. putida* PCA) and the sensor strain (*P. putida* SENS) in DBM medium with 20 mM glucose. In control experiments, the producer strain and wild-type *P. putida* KT2440 were individually grown in the same conditions. Wild-type *P. putida* KT2440 was also co-cultured with the SENS strain, which could not grow under these conditions. In all cases, results represent average values \pm standard deviations from three independent experiments.

Individual cultures of *P. putida* KT2440 (wild-type strain) and *P. putida* PCA, and a co-culture of *P. putida* KT2440 with *P. putida* SENS; all showed similar, low, fluorescence values (<5000 arbitrary units, Fig. 2D). The fluorescence background is expected because *P. putida* is known to display autofluorescence in the minimal medium due to siderophore excretion⁵⁵. These control experiments show that *P. putida* does not excrete any metabolites that can be used by the sensor

strain as a growth substrate. As expected, *P. putida* SENS did not grow as a pure culture under these conditions.

When *P. putida* PCA was co-cultured with *P. putida* SENS, we observed a fluorescence value > 3-fold higher than that of the *P. putida* PCA producer strain alone. The fluorescence profile ramped up shortly after the producer strain started growing, indicating that *P. putida* SENS can grow on PCA as soon as it is produced. TF-based biosensors

for this aromatic compound^{63,64} exhibit a logarithmic response (the output signal roughly doubles upon a 10-fold increase in the analyte concentration). In contrast, the growth-coupled approach illustrated here displayed a linear response. Our system is therefore a promising alternative to screen for high-titer producing strains in a high-throughput fashion as smaller differences in output can be detected. These results encouraged us to test the system for sensing metabolites produced by a different bacterial species.

Sensing D-lactate production by engineered *E. coli* with *P. putida* SENS-L

D-Lactate, a top value-added chemical with multiple industrial applications, can be produced by cell factories from a variety of feedstocks⁶⁵. Screening methods to select high-level producers often involve measuring the concentration of the acid in culture supernatants by chromatography⁶⁶, which limits the screening throughput. Hence, we explored if *P. putida* SENS could facilitate the detection and quantification of D-lactate produced by cell factories from glucose.

We first engineered *P. putida* SENS to be compatible with an *E. coli*-based production system for D-lactate. Since *E. coli* secretes acetate as an overflow metabolite when grown on sugars, the assimilation of this organic acid by *P. putida* SENS was blocked by deleting the isocitrate lyase gene (*aceA*, Fig. 1B). The resulting strain (Supplementary Table 1 and Fig. 1) was unable to grow on acetate as the only carbon substrate, whereas growth in DBM medium containing a permissive, gluconeogenic carbon source (succinate) was unaffected (Supplementary Fig. 3). We also disarmed *P. putida*'s type VI secretion system, used to attack other Gram-negative bacteria such as *E. coli*, by knocking-out *tssAI*, a gene essential for the system's activity⁶⁷ (Fig. 1B). We dubbed this new strain SENS-L.

Next, we asked if D-lactate can be quantified with *P. putida* SENS-L. We grew strain SENS-L without D-lactate, as a control, and with D-lactate at concentrations up to 20 mM. The maximum msfGFP signal increased up to 60-fold compared to the background fluorescence in the control experiment (Fig. 3B). We also identified a reproducible increase in the fluorescence signal (3-fold) at low D-lactate concentrations (0.15 mM, Fig. 3C), even when the sensitivity of the fluorescence detector was set to its lowest detection level. These results indicate that *P. putida* SENS-L can be used for detection of the acid over a 200-fold concentration range, with the msfGFP output linearly correlating with D-lactate concentration ($R^2 = 0.98$).

To implement *P. putida* SENS-L as a D-lactate-sensor strain in a biotechnology-relevant setup, we engineered *E. coli* for glucose-dependent D-lactate production. We first deleted the catabolic D-lactate dehydrogenase (*dld*) gene⁶⁸ to prevent D-lactate degradation (Fig. 3D). We then generated a combinatorial expression library comprising nine different constitutive promoters and nine regulatory elements (RBSs and bicistronic designs, BCDs⁶⁹) hooked up to the D-lactate dehydrogenase gene of *P. putida* KT2440 (*ldhA_PP*, *PP_1649*), in a low-copy-number vector⁷⁰ (Supplementary Tables 1 and 3). As a positive control strain, a highly active mutant of the LdhA dehydrogenase from *Bos taurus* (*BtldhA*^{N109G})⁷¹, expressed under the constitutive P_{tac} promoter (Supplementary Table 1), was introduced in *E. coli* Δdld . As a negative control strain, we transformed the same *E. coli* Δdld strain with an empty vector.

We next tested individual clones from our *E. coli* library for D-lactate production. We cultured *P. putida* SENS-L for 24 h in supernatants from *E. coli* clones grown in glucose-containing media, including supernatants from negative- and positive-control *E. coli* strains. The positive control experiment yielded an msfGFP signal 2-fold higher than background levels, while the negative control experiment yielded a fluorescence output within the background. The assays with supernatants from the *E. coli* library strains, in turn, yielded msfGFP levels above the background for all promoter and RBS combinations, over a 26-fold range (Fig. 3E). Seven *ldhA_PP* designs led to

msfGFP levels >10-fold higher than the negative control (Fig. 3E); the combination of the constitutive P_{EM7} promoter and the strong BCD1 translation coupler [$P_{EM7}(BCD1) \rightarrow ldhA_PP$] yielded the strongest fluorescence signal.

To validate these results with an independent analytical method, the D-lactate concentration in the supernatants was measured by HPLC (Supplementary Table 4). D-Lactate could not be detected in cultures of the negative control strain, whereas the positive control strain produced up to 0.7 mM D-lactate. The strain harboring the $P_{EM7}(BCD1) \rightarrow ldhA_PP$ design produced D-lactate to 4.7 mM, the highest titer among all the variants (Supplementary Table 4). A poor linear correlation between msfGFP fluorescence of *P. putida* SENS-L and HPLC quantification of D-lactate was observed ($R^2 = 0.48$, Fig. 3E). We note that D-lactate detection by HPLC was challenging due to the presence of other compounds that eluted closely with the target metabolite. The poor producer strains had a low fluorescence output, apart from three variants that yielded a higher fluorescence signal than expected for the low D-lactate levels detected. In contrast, the four best D-lactate producers gave the highest fluorescence signal among all variants. These results indicate that the sensor strain can be applied for screening of high-level D-lactate producers (>1.5 mM), which prompted us to further explore other potential applications, including monitoring plastic degradation processes.

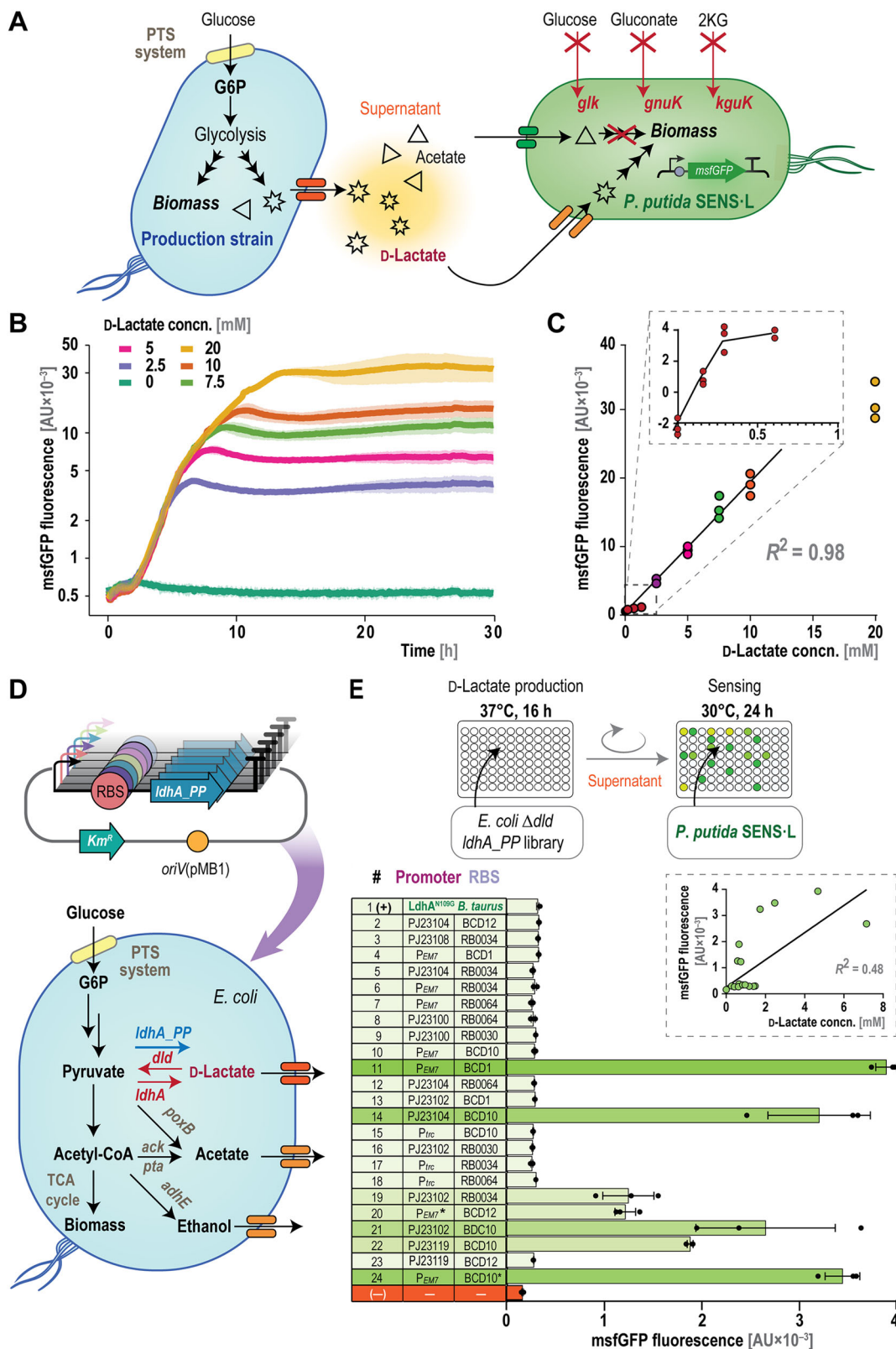
Engineering the SENS strain to detect PETase activity through terephthalate assimilation

Plastic pollution is a major environmental concern of our modern society. Polyethylene terephthalate (PET), for instance, accounts for ca. 12% of global solid waste and is predominantly managed through incineration. The potential for biological upcycling of PET materialized with the discovery of *Ideonella sakaiensis*, the first bacterium known to degrade PET^{72,73}. In a biological process for PET degradation, the initial depolymerization is catalyzed by either PETases or cutinases; the hydrolysis products are bis(2-hydroxyethyl) terephthalate (BHET), mono(2-hydroxyethyl) terephthalate (MHET), terephthalate (TPA), and ethylene glycol (EG) (Fig. 4A). These biological processes for plastic degradation are promising, but testing engineered and newly discovered hydrolytic enzymes and microbial strains remains tedious and time-consuming, since current methods have a limited throughput and capacity^{74–77}. We explored if WCB approaches have the potential to screen both enzymes and microbial strains for plastic degradation more effectively under different conditions.

The first step was to enable growth of the SENS strain on TPA, a PET hydrolysis product. To this end, we engineered the SENS strain to express the *tph* operon of *P. umsongensis*, a strain isolated from soil exposed to PET granules^{78,79}. This operon encodes the genes that convert TPA into PCA and another intermediate (1,2-dihydroxy-3,5-cyclohexadiene-1,4-dicarboxylic acid) (Fig. 4B); PCA can be assimilated by *P. putida* KT2440, with succinate and acetyl-coenzyme A as the final products⁸⁰. The engineered strain, bearing the pBT-T_{tph} plasmid, was dubbed *P. putida* SENS-T, and it grew on a minimal medium containing 2 g L⁻¹ TPA (Fig. 4C) with a high correlation between biomass formation and fluorescence output ($R^2 = 0.99$, Supplementary Fig. 4).

Since our WCB approach relies on biomass formation, faster growth would benefit the speed of screening based on *P. putida* SENS-T. Therefore, *P. putida* SENS-T was submitted to adaptive laboratory evolution with TPA as sole carbon and energy source. The specific growth rate doubled after only one week of evolution (up to 0.55 h⁻¹) and improved slightly in the following seven weeks to finally reach 0.64 h⁻¹ (Fig. 5A). The evolved TPA-sensor strain was termed *P. putida* SENS-TE (Supplementary Fig. 1).

Sequencing of the evolved strains revealed mutations in both the chromosome and the pBT-T_{tph} plasmid (Supplementary Table 5). The mutations in the chromosome of the evolved strain appear to be



general adaptations for faster growth in minimal medium⁸¹, with no direct association with TPA utilization (Supplementary Table 5). The evolved pBT-T_{tph} plasmid (pBT-T_{tph}^f) contained two mutations: one in an intergenic region of the backbone, and the other was an adenine-to-guanine transition at the -16 position upstream of *iclR*, an isocitrate lyase regulator (*IcLR*)-type gene⁸². We predicted that this mutation affects the RBS upstream *iclR* (Fig. 5B), and in silico analysis⁸³ estimated

a 24% increase in the translation initiation rate of *iclR*. Elevated levels of *IcLR* likely increase transcription of the *tph* genes. The adenine-to-guanine transition was reverse-engineered into the original sequence, giving rise to plasmid pBT-T_{tph}^M, which was introduced into the pre-evolved SENS strain. In parallel, the evolved pBT-T_{tph}^f plasmid was isolated and likewise introduced into the SENS strain. Both strains, carrying the evolved or reverse-engineered plasmid, grew on TPA with

Fig. 3 | Testing a library of *E. coli* strain engineered for D-lactate production with a *P. putida* sensor strain. **A** Screening high-titer D-lactate producers with a whole-cell biosensor. *E. coli* engineered for D-lactate production can grow on glucose, which cannot be utilized by the sensor strain (*P. putida* SENS-L). Assimilation of acetate by strain SENS-L, a major by-product of *E. coli*, was prevented by deleting *aceA*. D-Lactate is used by the sensor strain as the only growth substrate, coupling the D-lactate concentration (concn.) secreted by engineered *E. coli* to the fluorescent (msfGFP) output by *P. putida* SENS-L. Abbreviations are as indicated in the caption of Fig. 1. **B** Calibrating the growth and fluorescence output of the sensor SENS-L strain with respect to the D-lactate concn. The sensor strain was incubated in DBM medium supplemented with D-lactate at different concns.; the msfGFP signal was normalized to the cell density and plotted in semi-logarithmic scale over time. **C** Relationship between maximum msfGFP fluorescence by *P. putida* SENS-L and the D-lactate concn. The lowest range of analyte concns. (< 1 mM) is zoomed-in in the inset; the maximum D-lactate concn. quantifiable within the linearity range is highlighted in orange. **D** Engineering *E. coli* for D-lactate production from glucose.

Product degradation was prevented by deleting *ddd*, and a combinatorial library of constitutive promoters and ribosome binding sites (RBS), regulate the expression of *ldhA_PP*, a D-lactate dehydrogenase gene from *P. putida*, was introduced in the *E. coli* Δdld strain. **E** Exploiting *P. putida* SENS-L to screen for high-titer D-lactate producers. *E. coli* Δdld , carrying the combinatorial *ldhA_PP* library, was grown on M9 minimal medium with 20 mM glucose; individual culture supernatants were transferred to a new microtiter plate, inoculated with *P. putida* SENS-L and incubated for 24 h. Normalized fluorescence signals by strain SENS-L are shown for selected promoter and RBS combinations. The culture supernatant of *E. coli* Δdld carrying a plasmid with constitutive expression of a mutant version of the *ldhA* from *Bos taurus* was used as a positive control (+); the negative control (-) consisted of the same *E. coli* strain carrying an empty plasmid. In all cases, results represent average values \pm standard deviations from three independent experiments. The inset shows the relationship between D-lactate quantification *via* msfGFP fluorescence with the sensor strain and HPLC for all experimental samples.

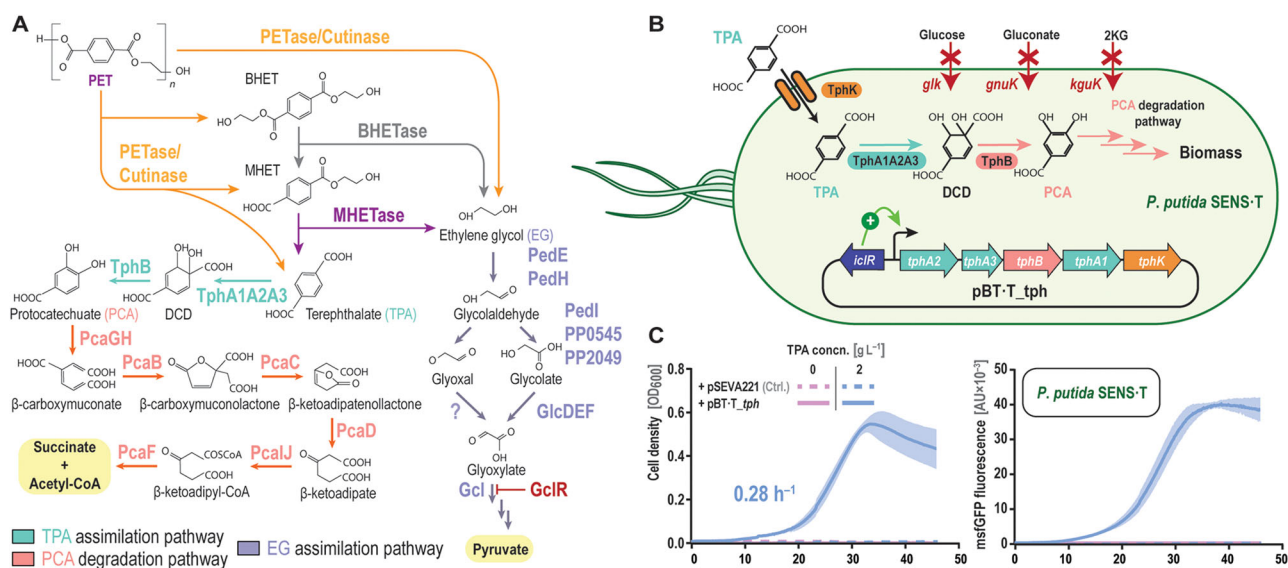


Fig. 4 | Engineering TPA assimilation in *P. putida* SENS. **A** Polyethylene terephthalate (PET) can be degraded by hydrolytic enzymes (for instance, PETases and cutinases). Metabolites resulting from these enzymatic reactions are BHET, bis(2-hydroxyethyl) terephthalate; MHET, mono(2-hydroxyethyl) terephthalate; TPA, terephthalate; and EG, ethylene glycol. MHET can be converted into TPA and EG by MHETase; this enzyme also displays residual activity on BHET, yielding MHET and EG. Abbreviations: CoA, coenzyme A; DCD, 1,6-dihydroxycyclohexa-2,4-diene-dicarboxylate. **B** The *tph* operon from *P. umsongensis*, encoded in plasmid pBT-T_tph, enables TPA transport and catabolism in *P. putida* SENS-T. The *tph* operon encodes an IclR-type regulator (regulating the expression of the remaining

genes in the cluster), the TPA 1,2-dioxygenase subunits α (*tphA2*) and β (*tphA3*), a reductase (*tphA1*), a dehydrogenase (*tphB*), and a TPA transporter (*tphK*). These activities convert TPA into protocatechuate (PCA). PCA is assimilated by *P. putida* through its conversion into succinate and acetyl-CoA. **C** Assessing TPA assimilation by the sensor *P. putida* SENS-T strain. *P. putida* SENS was transformed with either the pBT-T_tph plasmid or an empty vector (pSEVA221). The resulting strains were incubated in DBM medium supplemented with 2 g L⁻¹ TPA as the only carbon substrate. Growth and msfGFP fluorescence profiles are shown as average values \pm standard deviation of three independent experiments. Abbreviations: AU, arbitrary units.

$\mu = 0.57 \text{ h}^{-1}$ (Fig. 5C), similarly to the evolved strain. Furthermore, a reduction in the lag phase was apparent with both strains, likely caused by a higher basal expression of the *tph* operon.

We next tested the capacity of the evolved strain *P. putida* SENS-TE to sense TPA. The strain grew quickly on varying concentrations of TPA and gave a stable fluorescent output (Fig. 5D), which correlated linearly with the TPA concentration. Even though the sensitivity of the plate reader was set at low gain, a 2-fold signal increase over the background was verified at concentrations as low as 156 μM TPA (Fig. 5E). The response of SENS-TE was linear over the entire concentration range ($R^2 = 0.97$, Fig. 5E), with an 80-fold change in the msfGFP fluorescence, indicating a wide sensitivity and operational range. These results compare favorably with TF-based biosensors reported in the literature. One such biosensor, for instance, had a maximum 7-fold increase in fluorescence when exposed to 10 mM TPA⁸⁴. Our results prompted us to explore other formats for sensing PET degradation.

Engineering the SENS-T strain to quantify enzymatic PET depolymerization

We reasoned that the sensor *P. putida* strain could be applied to assess enzyme activity, offering an opportunity for high-throughput screening of variants and treatment conditions^{85,86}. The major products of most PET-degrading enzymes are MHET and BHET, which slowly degrade to TPA and EG by the enzymes themselves or MHETases (a MHET hydrolase from *I. sakaiensis*, Fig. 4A). To enhance the sensitivity of our WCB setup, we sought to engineer the evolved SENS-TE strain to degrade MHET (Fig. 6A). To this end, we inserted a codon-optimized version of the MHETase from *I. sakaiensis* together with its native secretion signal⁸⁷ into the genome of *P. putida* SENS-TE using a mini-Tn5 transposase (Supplementary Table 1 and 6). The strain variant with fastest growth on MHET (Supplementary Table 1 and Fig. 5) was dubbed *P. putida* SENS-TM and selected for further engineering.

Enabling EG assimilation in the sensor strain would further increase the amount of accessible carbon substrate (Fig. 6A) and

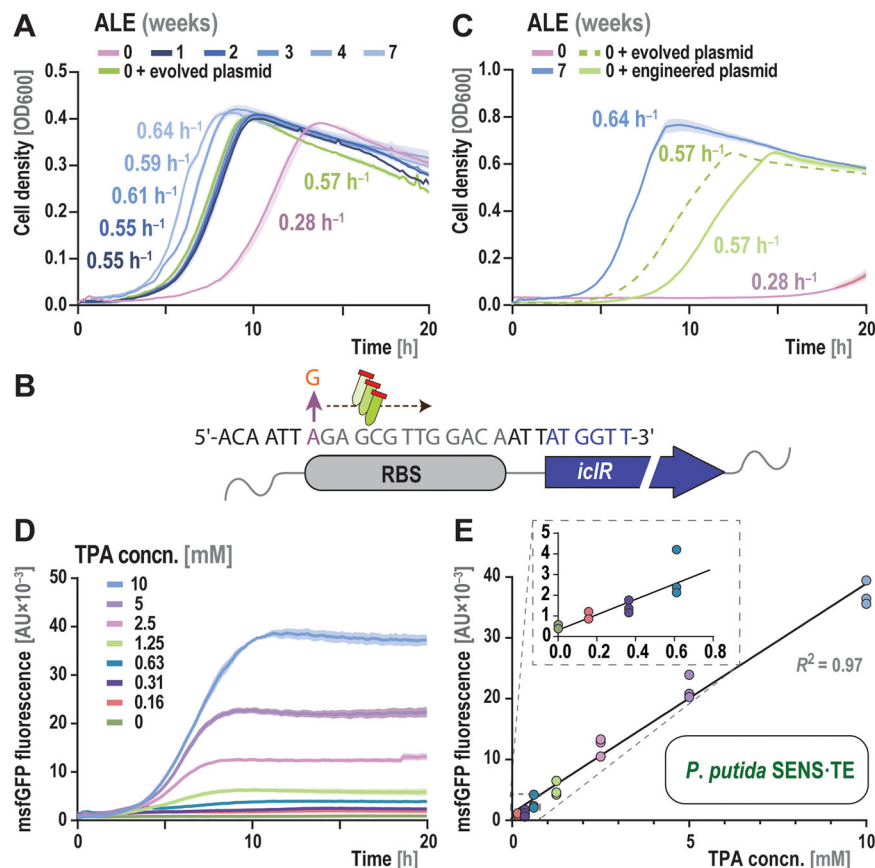


Fig. 5 | Adaptive laboratory evolution improves TPA detection by the sensor *P. putida* SENS-T strain. **A** Growth profile of the sensor *P. putida* SENS-T strain and its derivatives isolated at different points during adaptive laboratory evolution (ALE) in DBM medium with 1 g L^{-1} TPA. The naïve (pre-evolution) SENS strain was retransformed with plasmid pBT-T_{tpH}^E, isolated from the strain that underwent 7 weeks of ALE (indicated as *evolved plasmid*). **B** Physical map of the *iclR* locus of *P. umsongensis*, highlighting the mutation detected in the evolved plasmid pBT-T_{tpH}^E upon sequencing after ALE. **C** Growth profile of the sensor *P. putida* strain before (SENS-T) and after ALE (SENS-TE), compared to the naïve strain transformed with the evolved and reverse-engineered plasmid pBT-T_{tpH}^M, carrying an A-to-G

transition at -16 nt of *iclR* (indicated as *engineered plasmid*). All strains were grown in DBM medium supplemented with 2 g L^{-1} TPA. **D** msfGFP fluorescence profile of the sensor *P. putida* SENS-TE strain grown in DBM medium with increasing TPA concentrations (concn.). **E** Relationship between maximum msfGFP fluorescence by the sensor *P. putida* SENS-TE and the TPA concn. in the medium. The lowest range of analyte concns. ($< 1 \text{ mM}$) is zoomed-in in the inset; the maximum TPA concn. quantifiable within the linearity range is highlighted in light blue. In all cases, growth and msfGFP fluorescence profiles are shown as average values \pm standard deviation of three independent experiments. Abbreviations: AU, arbitrary units.

reduce glycolaldehyde accumulation as a toxic intermediate resulting from partial EG catabolism⁸⁸. Hence, we generated a SENS-TM strain capable of assimilating EG. The only essential modification needed in *P. putida* to awaken EG utilization is blocking the activity of the GclR regulator⁸⁹, which represses the *gcl* operon responsible for glyoxylate catabolism⁹⁰ (Fig. 4A). We inactivated *gclR* by CRISPR base-editing⁵⁴ in the SENS-TM strain, enabling growth on EG (Supplementary Fig. 6). The fully engineered strain (termed *P. putida* SENS-P), expressing *MHETase* and able to utilize EG, should more sensitively detect PET breakdown. The assimilation of EG and MHET by *P. putida* SENS-P was explored by incubating the strain with 10 mM TPA and varying amounts of each substrate; strain SENS-TE was included as a control. While the growth of *P. putida* SENS-TE was not affected by the presence of either PET degradation product, strain SENS-P showed an increase in biomass and fluorescence depending on the amount of EG and MHET supplemented (Fig. 6B).

We implemented *P. putida* SENS-P to quantify enzymatic PET degradation by the leave and branch compost cutinase (LCC)⁹¹ in a two-stage process. In the first stage, PET particles were incubated with LCC under a range of conditions to be screened for optimal degradation. We tested varying temperatures (50 or 60°C), treatment times (7 or 24 h), and enzyme concentration (0.1 or $0.5 \mu\text{M}$). In the second stage, *P. putida* sensor strains were incubated on the supernatant of

the enzymatic reactions. We quantified all potential degradation products by inoculating strain SENS-P (TPA, MHET, and EG) and strain SENS-TE (TPA). We observed a 3-fold higher msfGFP signal across all assays when using the fully engineered SENS-P strain as compared to strain SENS-TE, which can only assimilate TPA (Fig. 6C).

We found that increasing the temperature during enzymatic treatment of PET roughly doubled plastic hydrolysis in all conditions (Fig. 6C), whereas a higher LCC concentration boosted degradation by 4-fold at 24 h . Extending the incubation time increased PET degradation across all conditions. Assessing PET degradation with our sensor *P. putida* strains correlated well with the TPA and MHET concentrations measured in the samples by HPLC (Fig. 6D). Using the two sensor strains allowed us to distinguish the different degradation products; MHET was the main product in all conditions, followed by TPA and BHET (Supplementary Fig. 7 and 8).

The sensor strains had a sensitivity sufficient to detect enzyme activity under all the conditions tested, even when TPA and MHET were released at very low ($< 50 \mu\text{M}$) concentrations. Hence, the WCB system is suitable for in vitro screening of multiple conditions and enzyme variants. This setup has the potential to facilitate the assessment of variant libraries that previously could only be analyzed through time-consuming measurement of metabolites by HPLC. We next asked whether this approach could be extended to an in vivo setup.

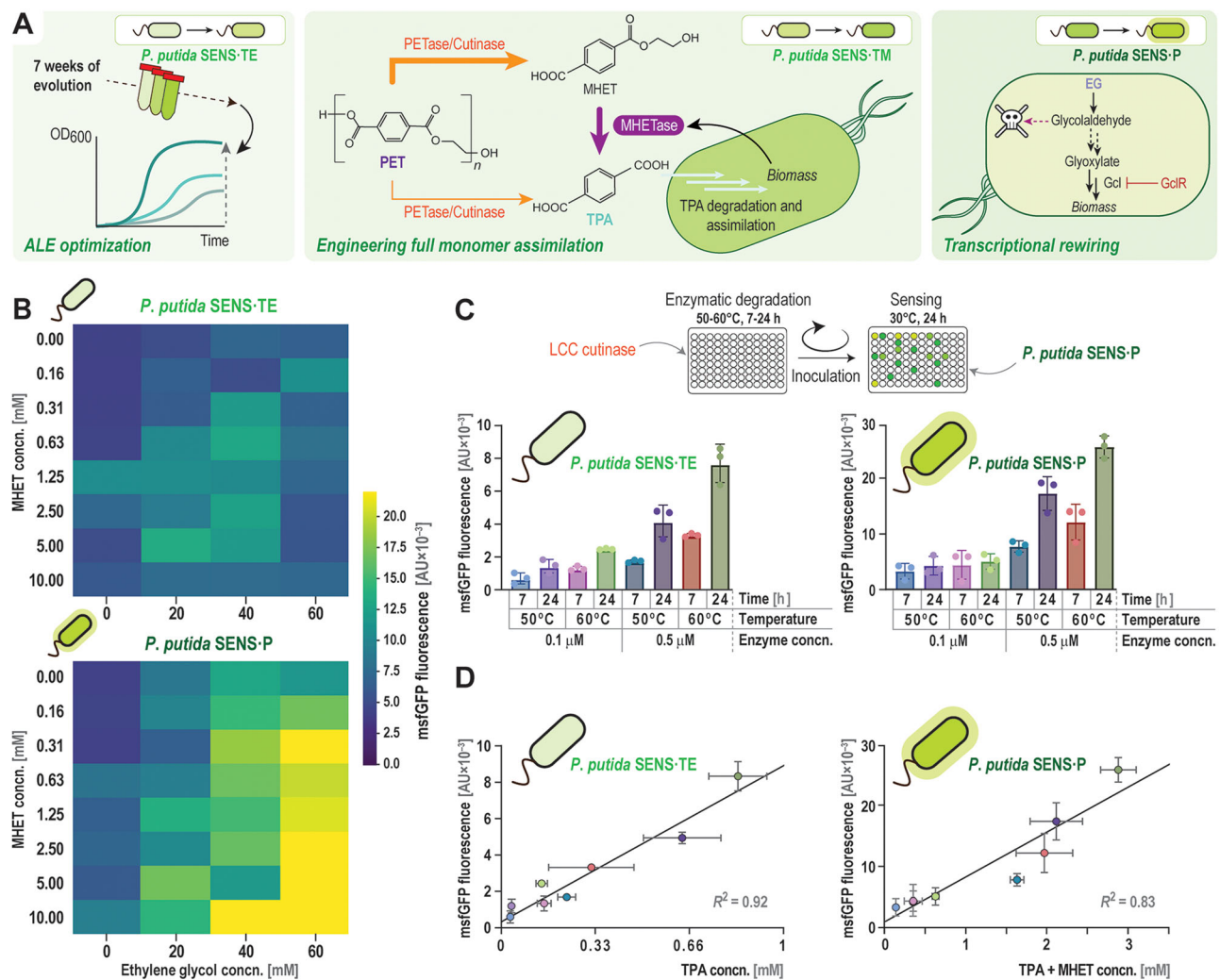


Fig. 6 | Construction of the sensor *P. putida* SENS-P strain for detecting PET-degradation products. **A** Enabling ethylene glycol (EG) and monohydroxyethyl terephthalate (MHET) assimilation to construct the sensor *P. putida* SENS-P strain. The growth of strain SENS-T was improved through adaptive laboratory evolution, yielding SENS-TE; subsequent genomic integration of a *MHEase* module enables constitutive production and secretion of this hydrolytic enzyme (*P. putida* SENS-TM). Deletion of the *gclR* regulator gene lifted the repression of the catabolic pathway that transforms glyoxylate into pyruvate, allowing for complete assimilation of PET-breakdown products; these modifications gave rise to strain SENS-P. **B** Combinatorial titration of MHET and EG for the sensor strains SENS-TE, which can only consume TPA, and SENS-P, engineered for MEHT and EG consumption. The

msfGFP fluorescence profile of the sensor strains was evaluated in DBM medium with 10 mM TPA and increasing MHET and EG concentrations (concn.). **C** A suspension of 20 g L⁻¹ PET was treated with the leaf and branch compost cutinase (LCC) at different enzyme concentrations (concn.), incubation times, and temperatures. After enzymatic treatment, the supernatant was inoculated with the sensor strain *P. putida* SENS-TE (left) or SENS-P (right). The msfGFP fluorescence signal was recorded after 24 h. **D** Relationship between the concentration of PET degradation products (TPA and MHET, independently quantified by HPLC) and the msfGFP fluorescence signal by sensor strain SENS-TE (left) and SENS-P (right). In all cases, results represent average values \pm standard deviation of three independent experiments. Abbreviations: AU, arbitrary units.

Using the SENS-P strain to characterize in vivo PET degradation by engineered *P. putida*

We next explored the application of the SENS-P strain to detect in vivo plastic breakdown in a co-culture system. In this setup, a plastic-degrading strain utilizes glucose as carbon and energy source, while the sensor strain grows on the degradation products released from PET by the PETase hydrolase (Fig. 7A). We engineered *P. putida* to constitutively express the *PETase* gene from *I. sakaiensis*⁷³ and secretion of the hydrolytic enzyme was established by fusing it to the porin F signal peptide, giving rise to *P. putida* PET-D (Fig. 7B). The PET-degrader strain was tested qualitatively by growing on minimal medium agar plates supplemented with BHET. *P. putida* PET-D generated clear halos surrounding the colonies after 7 days (Fig. 7B).

We next cultivated the PET-degrader strain together with *P. putida* SENS-P (Fig. 7C). No growth was detected in control experiments inoculated with the sensor strain alone, highlighting its dependence on a

plastic-degrading strain to release growth substrates. When co-cultured, the two strains had comparable growth rates and achieved similar cell densities. A significant increase in the msfGFP signal was observed when the co-culture was incubated with BHET, displaying a ca. 22-fold higher fluorescence level than the control experiment after 80 h (Fig. 7D). This fluorescence output was not observed in monocultures or in cocultures using glucose. The fluorescence began to increase around 18 h and continued to rise throughout the 80 h of incubation. The protracted msfGFP signal reflects the time needed for *P. putida* PET-D, the plastic-degrading strain, to grow first and provide the substrates for *P. putida* SENS-P, the sensor strain. Taken together, these results validate the use of WCB approaches for characterizing plastic degradation in vivo.

Discussion

In this work, we engineered *P. putida* as a widely applicable WCB by rendering several analytes of interest essential for growth through

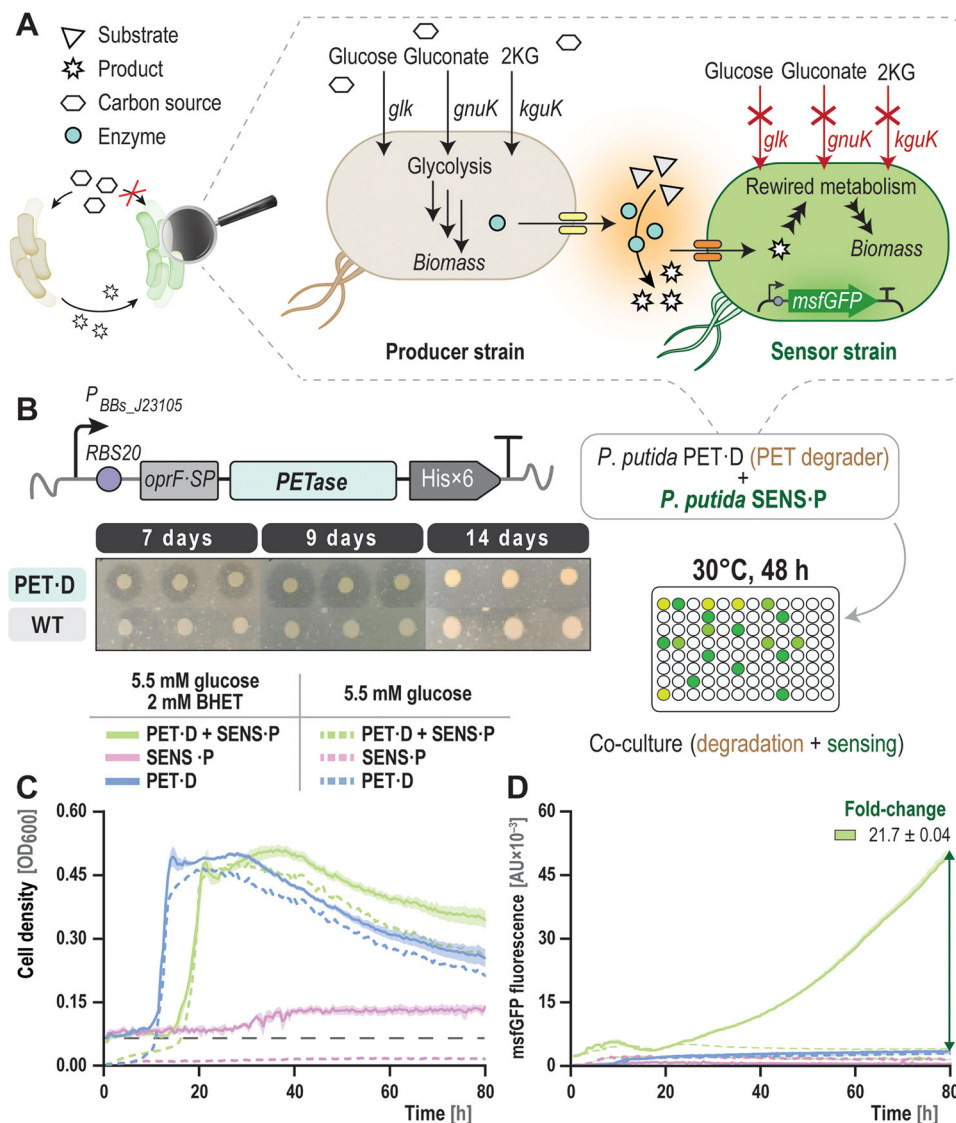


Fig. 7 | Characterizing microbial PET degradation by engineered bacteria with a growth-coupled, whole-cell *P. putida* sensor in a co-culture system. **A** Principle of the co-culture system for characterizing microbial PET degradation. The engineered PET-degrader strains (*P. putida* PET-D) secrete hydrolytic enzymes needed for PET breakdown into MHET, BHET, TPA, and EG; these metabolites can be utilized by the sensor strain (*P. putida* SENS-P) as carbon sources, yielding a fluorescent output proportional to the PET depolymerization capability of the corresponding degrader *P. putida* strain. **B** Genetic construct used to engineer PET-degrader strains. Microbial PET degradation was qualitatively tested by incubating wild-type (WT) *P. putida* KT2440 carrying an empty vector, and *P. putida* PET-D on AB medium agar plates supplemented with BHET for 14 days; clear halos around the

bacterial colonies are indicative of polymer breakdown. Three independent biological replicates are shown. **C** Growth profile of co-cultures performed with PET-degraders and the sensor strain. As control, *P. putida* PET-D and *P. putida* SENS-P were each cultivated alone. The AB medium was supplemented with 5.5 mM glucose with or without 2 mM BHET; the dashed gray line represents the background absorption by BHET in the medium. **D** msfGFP fluorescence profile of the co-cultures. The mean fold-change in fluorescence levels in the co-culture setup was calculated with respect to the control culture (PET-degrader only) at 80 h. In all cases, results represent average values \pm standard deviation of four independent experiments. Abbreviations: AU, arbitrary units.

metabolic rewiring. We demonstrated the versatility of the system by detecting structurally diverse molecules, including PCA, D-lactate, and PET-degradation products, by dedicated *P. putida* WCB strains across a range of operating conditions. The modular nature of this microbial sensing platform facilitates the future customization of WCB strains to detect additional target chemicals with only minimal genetic modifications. The general strategy mitigates several constraints inherent to conventional methods, which typically require redesigning a biosensor for each new analyte. Since the measurable outputs of the system are cell density (OD_{600}) and fluorescence, this approach does not require sophisticated equipment and simplifies implementing the test phase of the DBTLc. Our platform can also be exploited for high-throughput screening. A recent report outlines the implementation of

droplet-based screening using *Lactococcus lactis*, engineered to detect specific amino acids⁹², for selecting strains of lactic acid bacteria with enhanced glutamate and leucine production. Detection of molecules by transducer-based biosensors has also been demonstrated in a microdroplet format⁹³, expanding the potential applications of our system to ultra-high-throughput setups.

The sensitivity and selectivity of WCB strains can be tuned as needed. The desired sensitivity of a sensor strain depends on how much analyte is needed for building a certain amount of biomass^{94,95}. For example, the target metabolite could act as the sole carbon or nitrogen source or replenish an essential—but low-demand—metabolite in the biochemical network (for instance, dihydroxyacetone phosphate or succinyl-coenzyme A). The demand is markedly different

in these cases. The boundaries for each auxotrophy can be defined by partitioning the metabolism into a node that is only fed by the target analyte and another node that can be replenished by another substrate, enabling control over the sensitivity of the WCB.

The selectivity of a WCB is likewise adjustable. Again, any given metabolic node can be isolated from the rest of the metabolism to allow influx of one or more substrates that complement the synthetic auxotrophy. In general, having a larger auxotrophic node, where multiple pathways converge, will allow for more substrates to complement the auxotrophy. Unwanted complementation can be prevented by blocking either the uptake or metabolism of these substrates, as shown in this study for the hexose substrates of *P. putida*. Another option to avoid an unwanted complementation is to disconnect the metabolism of the substrate such that it can no longer complement the auxotrophy. In this case, the substrates can still be metabolized but cannot recover growth of the sensor strain. In our study, this approach is exemplified through the *aceA* deletion in *P. putida* SENS-L, such that acetate still served as an energy source but could not be used for synthesizing building blocks for biomass.

Three cases can be differentiated in the implementation of growth-coupled WCBs. Firstly, the chemical of interest can complement the auxotrophy through the native metabolism of the host. Thus, no engineering of the host is necessary, as illustrated in our study with PCA. Secondly, complementation of the auxotrophy can occur through expression of heterologous genes, shown here for detecting PET-degradation products through functional expression of the *tph* cluster. Thirdly, the chemical of interest could be a xenobiotic (virtually foreign to life, for example, polycyclic aromatic hydrocarbons). In this case, our WCB technology can be applied to identify and isolate catabolic pathways⁹⁶ (for instance, from metagenomes of contaminated sites) or engineered enzymes, thus wiring xenobiotics into the native metabolism. Two recent examples of this scenario are the degradation of fluoxetine⁹⁷ and Tris [2-amino-2-(hydroxymethyl)propane-1,3-diol]⁹⁸. Some of these examples are illustrated in Fig. 8, where the hierarchy of exogenous and endogenous metabolites of *P. putida* is used to show the potential of sensing structurally complex substrates. Engineering efforts are greatly aided by the growth-coupling nature of our approach, as evolution and selection help establish catabolic pathways, as long as they can be connected to biomass formation.

Existing resources can be harnessed to extend our approach to other microbial hosts and target analytes. Genome-wide knockout libraries, such as the Keio collection of *E. coli* mutants⁹⁹, can be sourced to establish synthetic auxotrophies. For the design of more complex synthetic auxotrophies, genome-scale metabolic reconstructions can be employed^{37,100,101}. For example, 213 essential metabolites have been identified for *E. coli*¹⁰², offering possibilities for coupling the presence of multiple analytes to bacterial growth. Moreover, databases on functional and molecular information of enzymes, predictive tools for protein function, and a wealth of in silico approaches for enzyme engineering^{103–105} are available to ease the design of metabolic shunts that wire any target analyte into the metabolism of sensor strains. While these prospects for implementation are attractive, the system displays some inherent limitations for specific sensing applications. Biologically inert chemicals, for instance, may only be detectable by other analytical means and remain unviable for this system. Also, samples containing a broad range of structurally similar compounds, such as lignocellulosic hydrolysates¹⁰⁶, might present a challenge for selectively sensing individual chemicals. Furthermore, sensing with bacterial WCBs can only occur under physiological conditions. Therefore, sensing chemicals in samples that require working at high temperatures (for instance, to ensure solubility¹⁰⁷) or containing high concentrations of toxins¹⁰⁸ either requires specialized microbial chassis¹⁰⁹ or is outside the functional range of this platform. Also, in co-culture production setups, the WCB could consume the product(s) it detects, potentially changing the behavior of the system. To avoid this

limitation, a delayed co-culture might be suitable, where the sensor strain is inoculated at a very low density to allow the production phase to proceed to almost completion before significant growth of the sensor strain is formed.

Importantly, considering that our approach links microbial growth with enzyme and pathway performance, high-throughput setups can be leveraged for the self-optimization of biocatalysts through adaptive laboratory evolution^{110–112}. Implementing this strategy could enhance the utility of growth-coupled WCBs, extending its application beyond testing to also support the build phase of the DBTLc.

Methods

Bacterial strains, plasmids, and culture conditions

The bacterial strains and plasmids used in this study are described in Supplementary Table 1. *E. coli* strains were routinely cultivated at 37 °C, *P. putida*-derived strains were incubated at 30 °C. Lysogeny broth (LB, containing 10 g L⁻¹ tryptone, 5 g L⁻¹ yeast extract, and 5 g L⁻¹ NaCl) was used for overnight (16 h) cultures and pre-cultures; these were cultivated in a MaxQ™ 8000 incubator (Thermo Fisher Scientific Co., Waltham, MA, USA) with constant agitation at 250 rpm. For substrate-dependent growth and sensing experiments, *P. putida* strains were cultivated in de Bont minimal (DBM) medium¹¹³, containing 3.88 g L⁻¹ K₂HPO₄, 1.63 g L⁻¹ NaH₂PO₄, 2 g L⁻¹ (NH₄)₂SO₄, and 0.1 g L⁻¹ MgCl₂ · 6H₂O, with the initial pH adjusted at 7.0. DBM medium was added with a trace elements solution¹¹⁴ [10 mg L⁻¹ ethylenediaminetetraacetic acid (EDTA), 2 mg L⁻¹ ZnSO₄ · 7H₂O, 1 mg L⁻¹ CaCl₂ · 2H₂O, 5 mg L⁻¹ FeSO₄ · 7H₂O, 0.2 mg L⁻¹ Na₂MoO₄ · 2H₂O, 0.2 mg L⁻¹ CuSO₄ · 5H₂O, 0.4 mg L⁻¹ CoCl₂ · 6H₂O, and 1 mg L⁻¹ MnCl₂ · 2H₂O] and carbon sources at the concentrations indicated in the text. In vivo PET hydrolysis experiments were carried out in AB medium¹¹⁵, containing 2 g L⁻¹ (NH₄)₂SO₄, 6 g L⁻¹ Na₂HPO₄, 3 g L⁻¹ KH₂PO₄, 3 g L⁻¹ NaCl, 0.2 g L⁻¹ MgSO₄, 11 mg L⁻¹ Na₂SO₄, 10 mg L⁻¹ CaCl₂, and 5 mg L⁻¹ FeCl₃ · 7H₂O, with the carbon sources at the concentrations indicated in the text. When required, filter-sterilized antibiotic solutions were added at the following final concentrations (μg mL⁻¹): ampicillin, 100; gentamicin, 10; kanamycin, 50; and streptomycin, 100. Bacterial growth was assessed by measuring the OD₆₀₀; specific growth rates (μ) and other relevant kinetic growth parameters were calculated with the QurVe software¹¹⁶.

General DNA manipulations and plasmid construction

DNA spacers and oligonucleotides used in this study are listed in Supplementary Table 2. Commercial kits and enzymes were used according to the recommendations given by the corresponding manufacturers. Plasmid DNA and PCR amplicons were purified using the NucleoSpin™ plasmid EasyPure and NucleoSpin™ gel and PCR clean-up kits, respectively (Macherey-Nagel, Düren, Germany). PCR amplifications were performed using Phusion™ HotStart II high-fidelity or, in case the primers contained deoxyuracil residues, Phusion™ U Hot Start DNA polymerase (Thermo Fisher Scientific Co.). The *OneTaq*™ master mix (New England Biolabs, Ipswich, MA, USA) was used to perform colony PCRs. The USER enzyme (New England Biolabs) was used to carry out USER-cloning procedures. The DpnI restriction enzyme and T4 DNA ligase (Thermo Fisher Scientific Co.) were used according to standard protocols¹¹⁷. Mix2Seq™ kits (Eurofins Genomics GmbH, Ebersberg, Germany) were employed for routine Sanger sequencing.

Genomic DNA purification, library construction, and whole genome sequencing (WGS)

DNA of isolated clones was purified using the DNeasy™ Blood & Tissue Kit (Qiagen, Hilden, Germany) from 2 mL overnight cultures in LB. DNA was randomly sheared into short fragments of ca. 350 bp using ultrasonic interruption. Short and large DNA fragments were removed using magnetic bead size selection and subsequently verified by

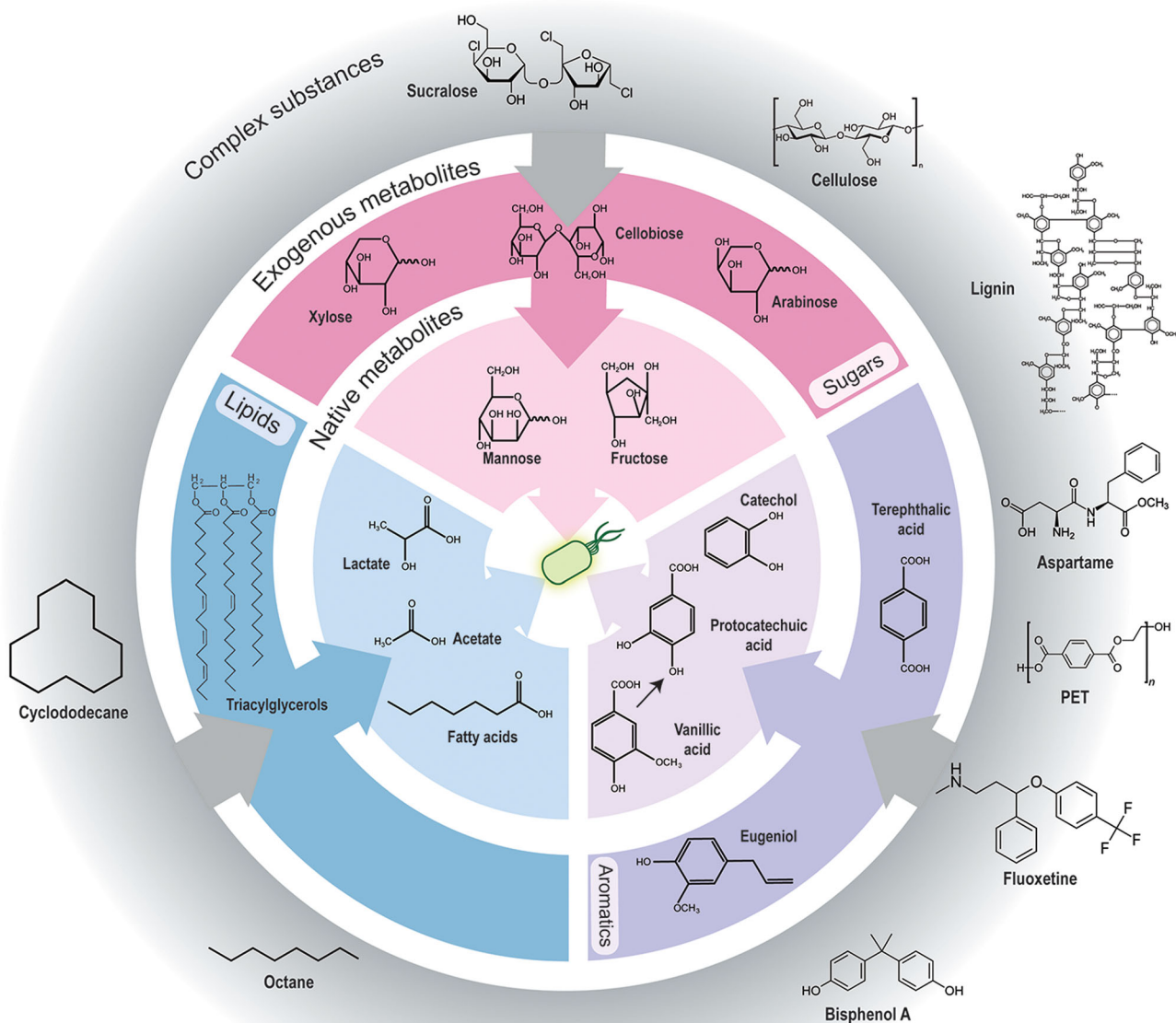


Fig. 8 | Examples of analytes amenable for growth-coupled sensing by engineered *P. putida*. All substances that can be metabolized to supply essential biomass precursors can theoretically be sensed. The diagram illustrates examples of chemicals that can serve as carbon and/or energy sources through their processing as sugars, organic acids, or aromatic molecules. Other essential nutrients could also be sensed using growth-couple WCBs, such as primary nitrogen and sulfur sources

or specific biomass components, for instance, amino acids. While native metabolites can be incorporated into the host metabolism without additional engineering, the range and chemical nature of analytes that can be sensed could be extended to exogenous or even complex substances, such as xenobiotics and complex polymers, through the metabolic engineering of the sensor strain.

capillary gel electrophoresis. The obtained DNA fragments were subjected to library construction using the NEBNext™ DNA Library Prep Kit (New England Biolabs), following the supplier's specifications. Libraries quality control was performed with a Qubit 2.0 fluorometer and an Agilent™ 2100 BioAnalyzer. Subsequent sequencing was performed using the Illumina NovaSeq™ 6000 PE150 platform. The original sequencing data acquired by high-throughput sequencing platforms recorded in image files were transformed to sequence reads by base calling with the Illumina's CASAVA software. Sequences and associated quality information were stored in a FASTQ file. For quality-control purposes, paired reads were discarded when: (i) either read contained adapter contamination, (ii) uncertain nucleotides (*N*) constituted >10% of either read, or (iii) low quality nucleotides (base quality ≤ 5) constituted > 50% of either read. The effective sequencing

data were aligned with the *P. putida* KT2440 reference sequence (GenBank, NC_002947), after error correction, trimming, and normalization through Geneious (Biomatters, New Zealand), and the mapping rate and coverage were counted according to the alignment results. Single nucleotide polymorphisms (SNPs) and InDels were detected in Geneious. Variant calling of single nucleotide polymorphisms (SNPs) and small insertions and deletions (indels) was performed with a variant frequency threshold of 0.4 on all samples. Additionally, a variant calling with a threshold of 0.1 was performed on a negative control sample (i.e., not subjected to base editing) to identify existing nucleotide polymorphisms in the parental strain. The construction of libraries, sequencing, and subsequent data quality control was performed by Novogene Co. Ltd. (Cambridge, United Kingdom).

Gene deletions and functional knockouts in *P. putida*

Well-established protocols were followed to perform the different genome and gene manipulations in *P. putida* KT2440 described in this study⁵⁵. In-frame, targeted gene deletions were carried out via homologous recombination or insertion of premature *STOP* codons by CRISPR base-editing⁵⁴. I-SceI-mediated recombination was used to perform gene deletions related to glucose uptake and processing (*gcd*, *gad*, *gtsABCD*, *glk*, *gntT*, *PP_0652*, *gnuK*, *kguT*, and *kguK*) and *aceA*. The corresponding suicide plasmid to eliminate each of these functions, derived from pGNW2 (Supplementary Table 1), was delivered into the cells by electroporating around 300 ng of plasmid DNA into 80 μ L of a freshly prepared suspension of electrocompetent *P. putida* cells. These were prepared by washing four times (by centrifugation and resuspension) the biomass resulting from 4 mL of an overnight culture with a 300 mM sucrose solution¹¹⁸. Electroporations were performed with a Gene Pulser XCell (Bio-Rad Laboratories Inc., Hercules, CA, USA) set to 2.5 kV, 25 μ F capacitance and 200 Ω resistance in a 2-mm gap cuvette. Individual colonies displaying positive co-integration events were isolated and transformed with the helper pQURE6-H plasmid⁵⁵. Cells were recovered in 1 mL of LB supplemented with 2 mM of 3-methylbenzoate (3-mBz) and incubated for at least 2 h at 30 °C; the suspension was then plated onto LB agar containing the corresponding antibiotic(s) and 3 mM 3-mBz to induce both plasmid replication and I-SceI expression. Positive clones were identified by colony PCR and verified by Sanger DNA sequencing. Finally, the auxiliary plasmid was cured from the resolved co-integrant by omitting 3-mBz in subsequent passages of the culture in LB with no selective pressure.

Functional knockouts of *gclR* and *tssAI* were created by introducing premature *STOP* codons in the corresponding reading frames via CRISPR base-editing. The relevant spacers were selected using the software CRISPy-web¹¹⁹, available online; sgRNAs were prepared by PCR amplification of the gRNA-Csy4 cassette of plasmid pEX128-gRNA using oligonucleotides targeting either *gclR* or *tssAI*. Once the PCR products had been verified by gel electrophoresis, the CRISPR base-editing plasmid was constructed using Golden Gate cloning, assembling together the different sgRNAs and the base-editing vector pMBEC6 as described elsewhere⁵⁴. Chemically competent *E. coli* cells were transformed with 3 μ L of the resulting mixture; non-fluorescent colonies were selected and screened via colony PCR. PCR fragments of the correct size were Sanger-sequenced to verify the correctness of the DNA assembly procedure, and the corresponding bacterial colonies were inoculated in selective LB for plasmid DNA isolation. Next, 200 ng of the purified plasmid were transformed into 80 μ L of freshly prepared electrocompetent *P. putida* cells; cells were recovered in 1 mL of LB for 3 h at 30 °C. In the case of *gclR* mutants, after recovery of the cells, all the biomass was washed and transferred into DBM minimal medium supplemented with 200 mM EG for mutant screening. After 48 h, or else once bacterial growth was visually detected, the cultures were streaked into LB agar plates. Colony PCR and DNA sequencing were performed to verify the integration of the desired mutation. Next, plasmid curing was performed by restreaking the cells on LB agar plates supplemented with 5% (w/v) sucrose; the curing procedure was repeated four times⁵⁴. For the screening of *tssAI* mutants, cells were directly plated onto selective LB agar plates, performing serial dilutions to isolate singles colonies. Then, colony PCR and DNA sequencing of the amplicons were performed to verify the integration of the *STOP* codon into the *tssAI* gene. Plasmid curing was performed by restreaking one of the isolated colonies onto LB agar plates supplemented with 5% (w/v) sucrose as described above.

Engineering *E. coli* for D-lactate production

E. coli Δ *dld2*::Km^R (Supplementary Table 1) was obtained from the Keio collection⁹⁹; single colonies were grown overnight in 5 mL of LB at 37 °C and 250 rpm. An aliquot of 100 μ L of this pre-culture was used to inoculate 10 mL of LB and grown under the same conditions until an OD₆₀₀ = 0.5 was reached. Then, cells were washed three times by

centrifugation at 4 °C and 1500 \times g and resuspending in 1 mL of 300 mM sucrose. In the final wash, the pellet was resuspended in 400 μ L of 300 mM sucrose, and electroporated with 100 ng of the helper pE-FLP plasmid at 1.8 kV. Cells were recovered at 30 °C for 1 h to be further plated on LB with ampicillin and incubated overnight at 30 °C. Singles colonies were streaked in duplicate on LB with or without antibiotics. After incubation overnight at 37 °C, kanamycin-sensitive colonies were selected and re-streaked in LB with ampicillin plate to confirm loss of the pE-FLP plasmid. A kanamycin- and ampicillin-sensitive colony (*E. coli* Δ *dld*) was isolated for further manipulations.

A library of plasmids was constructed for producing D-lactate by cloning the *ldhA* gene from *P. putida* together with different promoter sequences and RBSSs. Golden Gate DNA assembly used equimolar amount of pre-assembled Level 0 plasmids (pMCO-xx, Supplementary Table 1) with nine RBS motifs, nine promoter sequences, a kanamycin-resistance marker (pMCO-8-18), a strong transcriptional terminator (pMCO-5-Terminator), *oriV*(pMB1) (pMCO-Ori-MB1), and connectors (pMCO-1-Connector and pMCO-6-connector)¹²⁰. The *ldhA* gene from *P. putida* was amplified from genomic DNA extracted from strain KT2440 with primers 35 and 35 (Supplementary Table 2) and cloned into a Level 0 plasmid. Competent cells of *E. coli* DH5 α λ *pir* were transformed by heat-shock with the assembly mixture, recovered for 1 h at 37 °C in LB medium, and plated onto LB agar with kanamycin followed by an overnight incubation. Colony PCR was performed in single colonies with primers 38 and 39, and the resulting PCR amplicons were sent for sequencing. Among all the variants found in the library, 25 were randomly chosen for plasmid purification and were transformed into *E. coli* Δ *dld*. Plasmid pCJ015, carrying a mutant version of the *ldhA* gene from *Bos taurus*⁷¹, was used as a positive control. Next, single clones of *E. coli* Δ *dld* carrying the library were grown overnight in LB medium with kanamycin in 24-well plates. These cultures were washed twice with DBM medium without any carbon source by centrifuging the whole plate at 1500 \times g for 10 min, discarding the supernatant, and resuspending the cells in the same medium¹²¹. Fresh DBM medium supplemented with 20 mM glucose and 5 g L⁻¹ 3-(*N*-morpholino)propanesulfonic acid (MOPS) was then inoculated at an initial OD₆₀₀ = 0.1. The different clones were grown at 37 °C and 180 rpm in 24-well plates containing 2 mL of medium per well in triplicates. After 16 h of incubation, the cultures were centrifuged. An aliquot of 0.3 mL of the supernatant was used as the medium to incubate *P. putida* SENS-L in 96-well plates at 30 °C with continuous msfGFP fluorescence and OD₆₀₀ monitoring (Synergy HI BioTek, Agilent Technologies Inc., Santa Clara, CA, USA). In parallel, the concentration of D-lactate in a 0.1-mL aliquot of supernatant was quantified by HPLC. To this end, 10 μ L of the sample were injected into a Dionex Ultimate 3000 HPLC equipped with an Aminex™ HPX-87X Ion Exclusion (300 \times 7.8 mm) column (BioRad, Hercules, CA) as well as an UV detector. For analysis, the column was maintained at 50 °C and a 5 mM H₂SO₄ solution was used as the mobile phase at a flow rate of 0.6 mL min⁻¹. Lactate was quantified through its peak area at 205 nm through comparison to authentic standards. HPLC data were processed using the Chromeleon 7.1.3 software (Thermo Fisher Scientific), and compound concentrations were calculated from peak areas using calibration curves with five different standard concentrations.

Transposon-mediated genome integration in *P. putida*

Genes were stably integrated into the genome of *P. putida* KT2440 following different procedures as follows. The reporter *msfGFP* gene was inserted into the unique *attTn7* site of strain KT2440 with a Tn7 transposon borne by the pBG42 vector⁶⁰. The recipient strain was co-transformed with 200 ng of pBG42-*msfGFP* and 100 ng of the pTnS2 helper plasmid¹²². The transformed cells were plated onto selective LB agar plates, and fluorescent colonies were verified by colony PCR and amplicon sequencing. For the integration of the gene encoding the MHETase enzyme (Supplementary Table 6) in strain SENS-TE, Tn5-

mediated chromosomal insertion was achieved with plasmid pBAMD1-4-*MHETase*. For construction of the plasmids pBAMD1-4-*MHETase*, the codon optimized *MHETase* gene from *I. sakaiensis* (ISF6_0224; Twist Bioscience, San Francisco, CA, USA) was amplified with oligonucleotide 17 and 18, while pBAMD1-4 was amplified with primers 19 and 20 (Supplementary Table 2). The fragments were fused by USER cloning. Subsequently, the T₀ primer from the pSEVA collection was added in a similar fashion with primers 21–24. The plasmid pBAMD1-4-*MHETase* was introduced into *P. putida* by conjugation, mixing 500 μL each of an overnight culture of the recipient *P. putida* strain, *E. coli* DH5 α λpir containing plasmid pBAMD1-4-*MHETase*, and the helper *E. coli* HB101 strain carrying plasmid pRK600 (Supplementary Table 1). The bacterial mixture was washed three times with non-selective LB, and the biomass was recovered by centrifugation. The resulting pellet was resuspended in LB and the suspension was spotted onto LB agar plates, which were left open for 5 h in a laminar flow cabinet. After this incubation, cells were streaked onto selective LB agar plates containing 50 $\mu\text{g mL}^{-1}$ streptomycin and 25 $\mu\text{g mL}^{-1}$ 5-chloro-(2,4-dichlorophenoxy)phenol (IrgasanTM). These conjugation plates were incubated at 30 °C for 24 h for a second streaking procedure onto selective LB agar plates. Positive transconjugants were selected by growth on the selective solid medium and growth in liquid DBM medium containing 5 mM mono(2-hydroxyethyl)terephthalate (MHET).

Adaptive laboratory evolution

Overnight LB cultures of *P. putida* SENS transformed with plasmid pBT-T-*tph*⁷⁹ were washed and diluted 1:100 in DBM medium without any carbon source. This bacterial suspension was inoculated in 10 mL of DBM medium supplemented with 2 g L⁻¹ TPA and 50 $\mu\text{g mL}^{-1}$ kanamycin at an initial OD₆₀₀ = 0.05. Upon an extra overnight incubation at 30 °C, this pre-culture was used to start an adaptive laboratory evolution experiment by inoculating 10 mL of DB medium supplemented with the same additives at an initial OD₆₀₀ = 0.05. The working culture was serially passed at the same ratio into 10 mL of fresh medium with the same composition in 50-mL FalconTM tubes (Thermo Fisher Scientific Co.) every 2 days during the first 4 weeks of evolution. After 4 weeks, the cultures were transferred daily into fresh medium until the end of the evolution experiment (by the 7th week of cultivation, when no further phenotypic changes were recorded). In all cases, the cultures were grown at 30 °C and 250 rpm. Glycerol stocks were periodically prepared from the corresponding bacterial populations, and individual colonies were isolated from the evolved populations by the end of the experiment by plating the bacterial suspension onto selective LB agar plates. Upon confirming the relevant phenotypes, plasmid DNA purification and sequence analysis were used to identify mutations linked to enhanced TPA catabolism. Plasmid pBT-T-*tph*^M was created by site-directed mutagenesis through USER cloning with the primer pair 1 and 2 (Supplementary Table 2) on the original plasmid pBT-T-*tph*.

Enzymatic PET hydrolysis in vitro

The leaf-branch compost cutinase (LCC, E.C. 3.1.1.74, 293 amino acids) was employed as the hydrolytic enzyme for experiments involving in vitro PET degradation. The synthetic gene encoding LCC was heterologously expressed in *Bacillus subtilis*, and the recombinant enzyme was purified to homogeneity as described by Arnling Bååth et al.¹²³ The LCC concentration in purified preparations was estimated by measuring the absorbance at 280 nm and correlating these values with the actual enzyme concentration using ϵ^{LCC} , the theoretical extinction coefficient calculated for this enzyme¹²⁴. The substrate used in these assays consisted of a semicrystalline PET powder¹²⁵, purchased from Goodfellow Cambridge Ltd. (Huntingdon, UK; catalog # ES306031), with a reported molecular weight of 33 kDa and crystallinity of 38%. The PET powder was suspended in 50 mM sodium phosphate buffer (pH = 8.0) prior to the assays, and enzymatic

reactions were performed in triplicates in protein LoBindTM tubes (Sigma-Aldrich Co., St. Louis, MO, USA) with 0.1 or 0.5 μM LCC and 20 g L⁻¹ PET in a final volume of 500 μL . The enzymatic reactions were incubated at either 50 or 60 °C with constant agitation (1100 rpm) in an Eppendorf ThermomixerTM C platform (Eppendorf Nordic A/S, Hørsholm, Denmark) over 7 h or 24 h. Samples were removed at selected times and rapidly quenched by centrifugation; a 250 μL aliquot of the corresponding supernatants was stored at -20 °C for further analysis.

Engineering a *P. putida* strain (*P. putida* PET-D) for in vivo PET degradation

The gene encoding the PETase hydrolase from *I.*⁷³ was synthesized de novo by Twist Bioscience (San Francisco, CA, USA). The synthetic gene was cloned into the expression pSEVAb237 plasmid (Supplementary Table 1), bracketed with an N-terminal signal peptide from the porin F (*PP_2089*, *oprF*-SP) from *P. putida* KT2440 to facilitate secretion and a C-terminal His_{6x} tag (Supplementary Table 6); a synthetic transcriptional element composed of *P*_{BBSJ23105} and RBS20 was used to drive the constitutive expression of the PETase construct. The resulting plasmid was termed pSEVA-PET (Supplementary Table 1). All cloning steps were carried out by PCR assembly with the oligonucleotides specified in Supplementary Table 2 by using the NEBuilderTM HiFi DNA assembly master mix (New England Biolabs) and KAPATM HiFi PCR master mix (Roche Molecular Systems Inc., Indianapolis, IN, USA) following the specific manufacturer's instructions.

Analytical procedures

The products of PET enzymatic hydrolysis were analyzed using a Dionex UltiMate 3000 HPLC (Thermo Fisher Scientific Co.) equipped with an ZORBAX Eclipse AAA C18 reverse-phased column (4.6 \times 150 mm, 3.5 μm ; Agilent Technologies Inc., Santa Clara, CA, USA) as well as RI-150 refractive index and UV (210, 260, 277 and 304 nm) detectors. For the analysis of metabolites, the column was maintained at 30 °C and the mobile phase consisted of a gradient from 0.05% (v/v) acetic acid to 45% (v/v) acetonitrile at a low rate (1 mL min⁻¹); the starting pressure was 100 bar. D-Lactate detection was carried out under similar conditions, but an Aminex HPX-87H column (7.8 \times 300 mm, 9 μm ; Bio-Rad Laboratories Inc.) was used for separation instead. The column was maintained at 50 °C, with a typical running time of 30 min and using 5 mM H₂SO₄ as the mobile phase. In all cases, raw HPLC data were processed using the ChromeleonTM 7.1.3 software package (Thermo Fisher Scientific Co.), and metabolite concentrations were calculated from peak areas using calibration curves with eight different standard concentrations.

Concentration-dependent fluorescence assays

Growth of sensor *P. putida* strains on different carbon sources was assessed by incubating the cells in a Synergy HI microtiter plate reader (BioTek Instruments Inc., Winooski, VT, USA). In the case of growth on TPA (both for titration assays and for evaluating fitness improvement after evolution), 10 mM TPA was supplemented to DBM medium, either alone or together with variable concentrations of EG and MHET. Overnight cultures were prepared with the corresponding strains incubated in DBM medium supplemented with 5 mM (1 g L⁻¹) TPA and 50 $\mu\text{g mL}^{-1}$ kanamycin; these cultures were diluted 1:100 and distributed in 96-well microtiter plates. When assessing D-lactate-dependent growth; overnight cultures were prepared in DBM medium supplemented with 20 mM D-lactate. In all cases, bacterial cultures were incubated at 30 °C with constant orbital agitation. Measurements of OD₆₀₀ and msfGFP fluorescence ($\lambda_{\text{excitation}} = 485 \text{ nm}$ and $\lambda_{\text{emission}} = 528 \text{ nm}$) in microtiter plate reader were taken every 10 min over 24 h (BioTek Synergy HI, Agilent Technologies Inc., Santa Clara, CA, USA) unless specified otherwise in the text. The sensitivity of the plate reader was adjusted to a gain

between 50 and 100, depending on the expected maximum fluorescence.

Co-culture experiments for online monitoring PET hydrolysis by engineered *P. putida*

BHET medium was prepared by adding a filtered (0.22 µm) stock solution of 5% (w/v) glucose to AB medium (previously autoclaved) at a 1:10 ratio. A 10 mM BHET solution was prepared by grinding BHET flakes into small particles and heating at 70 °C for 1 h to pasteurize the resulting powder; posterior weighing was performed under aseptic conditions before adding the BHET powder to the AB medium⁸⁷. Next, co-cultures of *P. putida* SENS-P and *P. putida* PET-D were set as follows. Overnight cultures of the engineered strains were grown from isolated colonies from selective medium plates as indicated in the text. The overnight cultures were diluted to an initial OD₆₀₀ of 0.2, and a fresh culture in LB supplemented with kanamycin was incubated at 30 °C with shaking at 250 rpm until the OD₆₀₀ reached 0.8–1 (mid-exponential phase). Then, the cells were washed four times with AB medium with no carbon substrate, and the OD₆₀₀ of the bacterial suspension was adjusted to 0.5. The two suspensions (i.e., *P. putida* SENS-P and *P. putida* PET-D) were mixed at a 1:1 ratio (initial OD₆₀₀ of 0.025) in AB medium supplemented with 5 mM glucose, 2 mM BHET, and kanamycin, and the resulting bacterial culture was distributed in 96-well plates. Cultures were incubated at 30 °C with constant orbital agitation; OD₆₀₀ and msfGFP fluorescence ($\lambda_{excitation} = 485$ nm and $\lambda_{emission} = 528$ nm) were measured every 30 min over a total cultivation time of 80 h. Three biological replicates with four technical replicates were performed for each experiment. A control experiment, used to quantify auto-fluorescence levels for normalization, was performed using the sensor strain (*P. putida* SENS-P) inoculated as a monoculture.

Data and statistical analysis

All the experiments reported were independently repeated at least three times (as indicated in the corresponding figure or table legend), and the mean value of the corresponding parameter \pm standard deviation is presented unless indicated otherwise. In some cases, the level of significance of the differences when comparing results were evaluated by means of the Student's *t* test with $\alpha = 0.01$ or $\alpha = 0.05$ as indicated in the figure legends. Data analysis was performed with MS Excel™ (Microsoft Corp., Redmond, WA, USA) and Prism 8 (GraphPad Software Inc., San Diego, CA, USA) unless differently specified.

Reporting summary

Further information on research design is available in the Nature Portfolio Reporting Summary linked to this article.

Data availability

The datasets generated and analyzed in the current study are included in the paper and its Supplementary Information. The plasmids created in this work can also be requested through Addgene [https://www.addgene.org/Pablo_Nikel/]. The raw microbial sequencing data derived from this study has been deposited in the NCBI SRA database under accession number [SRR30677106](https://www.ncbi.nlm.nih.gov/nuccore/SRR30677106). Genome assembly data has been deposited in NCBI under accession number [CP167163.1](https://www.ncbi.nlm.nih.gov/nuccore/CP167163.1) [<https://www.ncbi.nlm.nih.gov/nuccore/CP167163>]. Source data are provided with this paper.

References

- Gurdo, N., Volke, D. C. & Nikel, P. I. Merging automation and fundamental discovery into the design–build–test–learn cycle of nontraditional microbes. *Trends Biotechnol.* **40**, 1148–1159 (2022).
- Carbonell, P. et al. An automated Design-Build-Test-Learn pipeline for enhanced microbial production of fine chemicals. *Commun. Biol.* **1**, 66 (2018).
- Cho, J. S., Kim, G. B., Eun, H., Moon, C. W. & Lee, S. Y. Designing microbial cell factories for the production of chemicals. *JACS Au* **2**, 1781–1799 (2022).
- Cai, J. et al. Designing gene manipulation schedules for high throughput parallel construction of objective strains. *Biotechnol. J.* **18**, e2200578 (2023).
- Ko, Y. S. et al. Tools and strategies of systems metabolic engineering for the development of microbial cell factories for chemical production. *Chem. Soc. Rev.* **49**, 4615–4636 (2020).
- Orsi, E., Schada von Borzyskowski, L., Noack, S., Nikel, P. I. & Lindner, S. N. Automated in vivo enzyme engineering accelerates biocatalyst optimization. *Nat. Commun.* **15**, 3447 (2024).
- Lawson, C. E. et al. Machine learning for metabolic engineering: a review. *Metab. Eng.* **63**, 34–60 (2021).
- Gurdo, N., Volke, D. C., McCloskey, D. & Nikel, P. I. Automating the design-build-test-learn cycle towards next-generation bacterial cell factories. *New Biotechnol.* **74**, 1–15 (2023).
- Deal, C., De Wannemaeker, L. & De Mey, M. Towards a rational approach to promoter engineering: understanding the complexity of transcription initiation in prokaryotes. *FEMS Microbiol. Rev.* **48**, fuae004 (2024).
- Lammens, E. M., Nikel, P. I. & Lavigne, R. Exploring the synthetic biology potential of bacteriophages for engineering non-model bacteria. *Nat. Commun.* **11**, 5294 (2020).
- Wirth, N. T. & Nikel, P. I. Combinatorial pathway balancing provides biosynthetic access to 2-fluoro-*cis,cis*-muconate in engineered *Pseudomonas putida*. *Chem. Catal.* **1**, 1234–1259 (2021).
- Leavell, M. D., Singh, A. H. & Kaufmann-Malaga, B. B. High-throughput screening for improved microbial cell factories, perspective and promise. *Curr. Opin. Biotechnol.* **62**, 22–28 (2020).
- Dietrich, J. A., McKee, A. E. & Keasling, J. D. High-throughput metabolic engineering: advances in small-molecule screening and selection. *Annu. Rev. Biochem.* **79**, 563–590 (2010).
- Kaczmarek, J. A. & Prather, K. L. J. Effective use of biosensors for high-throughput library screening for metabolite production. *J. Ind. Microbiol. Biotechnol.* **48**, kuab049 (2021).
- O'Connor, E., Micklefield, J. & Cai, Y. Searching for the optimal microbial factory: high-throughput biosensors and analytical techniques for screening small molecules. *Curr. Opin. Biotechnol.* **87**, 103125 (2024).
- Bayer, T., Hänel, L., Husarcikova, J., Kunzendorf, A. & Bornscheuer, U. T. In vivo detection of low molecular weight platform chemicals and environmental contaminants by genetically encoded biosensors. *ACS Omega* **8**, 23227–23239 (2023).
- Zhang, J., Jensen, M. K. & Keasling, J. D. Development of biosensors and their application in metabolic engineering. *Curr. Opin. Chem. Biol.* **28**, 1–8 (2015).
- Li, S., Li, Z., Tan, G. Y., Xin, Z. & Wang, W. In vitro allosteric transcription factor-based biosensing. *Trends Biotechnol.* **41**, 1080–1095 (2023).
- Snoek, T. et al. An orthogonal and pH-tunable sensor-selector for muconic acid biosynthesis in yeast. *ACS Synth. Biol.* **7**, 995–1003 (2018).
- Yang, L. F., Ling, M., Kacherovsky, N. & Pun, S. H. Aptamers 101: aptamer discovery and in vitro applications in biosensors and separations. *Chem. Sci.* **14**, 4961–4978 (2023).
- Wan, X., Saltepe, B., Yu, L. & Wang, B. Programming living sensors for environment, health and biomanufacturing. *Microb. Biotechnol.* **14**, 2334–2342 (2021).
- Goñi-Moreno, A. & Nikel, P. I. High-performance biocomputing in synthetic biology-integrated transcriptional and metabolic circuits. *Front. Bioeng. Biotechnol.* **7**, 40 (2019).
- Calero, P. et al. A fluoride-responsive genetic circuit enables in vivo biofluorination in engineered *Pseudomonas putida*. *Nat. Commun.* **11**, 5045 (2020).

24. Gonzalez-Flo, E., Alaball, M. E. & Macia, J. Two-component biosensors: unveiling the mechanisms of predictable tunability. *ACS Synth. Biol.* **9**, 1328–1335 (2020).
25. Yang, D. et al. Repurposing type III polyketide synthase as a malonyl-CoA biosensor for metabolic engineering in bacteria. *Proc. Natl Acad. Sci. USA* **115**, 9835–9844 (2018).
26. Chiang, A. J. & Hasty, J. Design of synthetic bacterial biosensors. *Curr. Opin. Microbiol.* **76**, 102380 (2023).
27. Feng, J. et al. A general strategy to construct small molecule biosensors in eukaryotes. *eLife* **4**, e10606 (2015).
28. Dietrich, J. A., Shis, D. L., Alikhani, A. & Keasling, J. D. Transcription factor-based screens and synthetic selections for microbial small-molecule biosynthesis. *ACS Synth. Biol.* **2**, 47–58 (2013).
29. Leavitt, J. M. et al. Biosensor-enabled directed evolution to improve muconic acid production in *Saccharomyces cerevisiae*. *Biotechnol. J.* **12**, 1600687 (2017).
30. Raman, S., Rogers, J. K., Taylor, N. D. & Church, G. M. Evolution-guided optimization of biosynthetic pathways. *Proc. Natl Acad. Sci. USA* **111**, 17803–17808 (2014).
31. Rennig, M. et al. TARSyn: tunable antibiotic resistance devices enabling bacterial synthetic evolution and protein production. *ACS Synth. Biol.* **7**, 432–442 (2018).
32. Copley, S. D. Evolution of efficient pathways for degradation of anthropogenic chemicals. *Nat. Chem. Biol.* **5**, 559–566 (2009).
33. Janssen, D. B., Dinkla, I. J., Poelarends, G. J. & Terpstra, P. Bacterial degradation of xenobiotic compounds: evolution and distribution of novel enzyme activities. *Environ. Microbiol.* **7**, 1868–1882 (2005).
34. de Lorenzo, V., Pérez-Pantoja, D. & Nikel, P. I. *Pseudomonas putida* KT2440: the long journey of a soil-dweller to become a synthetic biology chassis. *J. Bacteriol.* **206**, e00136–24 (2024).
35. Orsi, E., Claassens, N. J., Nikel, P. I. & Lindner, S. N. Growth-coupled selection of synthetic modules to accelerate cell factory development. *Nat. Commun.* **12**, 5295 (2021).
36. von Kamp, A. & Klamt, S. Growth-coupled overproduction is feasible for almost all metabolites in five major production organisms. *Nat. Commun.* **8**, 15956 (2017).
37. Schneider, P., Mahadevan, R. & Klamt, S. Systematizing the different notions of growth-coupled product synthesis and a single framework for computing corresponding strain designs. *Biotechnol. J.* **16**, e2100236 (2021).
38. Cros, A., Alfaro-Espinoza, G., de Maria, A., Wirth, N. T. & Nikel, P. I. Synthetic metabolism for biohalogenation. *Curr. Opin. Biotechnol.* **74**, 180–193 (2022).
39. Wenk, S., Yishai, O., Lindner, S. N. & Bar-Even, A. An engineering approach for rewiring microbial metabolism. *Methods Enzymol.* **608**, 329–367 (2018).
40. Alter, T. B. & Ebert, B. E. Determination of growth-coupling strategies and their underlying principles. *BMC Bioinformatics* **20**, 447 (2019).
41. Aslan, S., Noor, E., Benito Vaquerizo, S., Lindner, S. N. & Bar-Even, A. Design and engineering of *E. coli* metabolic sensor strains with a wide sensitivity range for glycerate. *Metab. Eng.* **57**, 96–109 (2020).
42. Turlin, J., Dronsella, B., De Maria, A., Lindner, S. N. & Nikel, P. I. Integrated rational and evolutionary engineering of genome-reduced *Pseudomonas putida* strains promotes synthetic formate assimilation. *Metab. Eng.* **74**, 191–205 (2022).
43. Dinh, H. V., King, Z. A., Palsson, B. Ø. & Feist, A. M. Identification of growth-coupled production strains considering protein costs and kinetic variability. *Metab. Eng. Commun.* **7**, e00080 (2018).
44. Banerjee, D. & Mukhopadhyay, A. Perspectives in growth production trade-off in microbial bioproduction. *RSC Sustain* **1**, 224–233 (2023).
45. Liu, C. et al. Engineering whole-cell microbial biosensors: design principles and applications in monitoring and treatment of heavy metals and organic pollutants. *Biotechnol. Adv.* **60**, 108019 (2022).
46. Moraskie, M. et al. Microbial whole-cell biosensors: current applications, challenges, and future perspectives. *Biosens. Bioelectron.* **191**, 113359 (2021).
47. Sahu, S., Ramachandran, S., Bandyopadhyaya, R. & Anand, R. Biosensing of multiple aromatic xenobiotics in water by in-house fabricated prototype device. *Biosens. Bioelectron.* **250**, 116077 (2024).
48. Ali, S. A., Mittal, D. & Kaur, G. In-situ monitoring of xenobiotics using genetically engineered whole-cell-based microbial biosensors: recent advances and outlook. *World J. Microbiol. Biotechnol.* **37**, 81 (2021).
49. Martínez-García, E. & de Lorenzo, V. *Pseudomonas putida* as a synthetic biology chassis and a metabolic engineering platform. *Curr. Opin. Biotechnol.* **85**, 103025 (2024).
50. Nikel, P. I., Chavarría, M., Fuhrer, T., Sauer, U. & de Lorenzo, V. *Pseudomonas putida* KT2440 strain metabolizes glucose through a cycle formed by enzymes of the Entner-Doudoroff, Embden-Meyerhof-Parnas, and pentose phosphate pathways. *J. Biol. Chem.* **290**, 25920–25932 (2015).
51. Belda, E. et al. The revisited genome of *Pseudomonas putida* KT2440 enlightens its value as a robust metabolic chassis. *Environ. Microbiol.* **18**, 3403–3424 (2016).
52. Nikel, P. I., Martínez-García, E. & de Lorenzo, V. Biotechnological domestication of pseudomonads using synthetic biology. *Nat. Rev. Microbiol.* **12**, 368–379 (2014).
53. Wirth, N. T., Kozaeva, E. & Nikel, P. I. Accelerated genome engineering of *Pseudomonas putida* by I-SceI—mediated recombination and CRISPR-Cas9 counterselection. *Microb. Biotechnol.* **13**, 233–249 (2020).
54. Volke, D. C., Martino, R. A., Kozaeva, E., Smania, A. M. & Nikel, P. I. Modular (de)construction of complex bacterial phenotypes by CRISPR/nCas9-assisted, multiplex cytidine base-editing. *Nat. Commun.* **13**, 3026 (2022).
55. Volke, D. C., Friis, L., Wirth, N. T., Turlin, J. & Nikel, P. I. Synthetic control of plasmid replication enables target- and self-curing of vectors and expedites genome engineering of *Pseudomonas putida*. *Metab. Eng. Commun.* **10**, e00126 (2020).
56. Martínez-García, E. et al. SEVA 4.0: an update of the standard European vector architecture database for advanced analysis and programming of bacterial phenotypes. *Nucleic Acids Res.* **51**, D1558–D1567 (2023).
57. Martínez-García, E., Aparicio, T., de Lorenzo, V. & Nikel, P. I. New transposon tools tailored for metabolic engineering of Gram-negative microbial cell factories. *Front. Bioeng. Biotechnol.* **2**, 46 (2014).
58. Nikel, P. I. et al. Reconfiguration of metabolic fluxes in *Pseudomonas putida* as a response to sub-lethal oxidative stress. *ISME J.* **15**, 1751–1766 (2021).
59. Volke, D. C., Gurdo, N., Milanese, R. & Nikel, P. I. Time-resolved, deuterium-based fluxomics uncovers the hierarchy and dynamics of sugar processing by *Pseudomonas putida*. *Metab. Eng.* **79**, 159–172 (2023).
60. Zobel, S. et al. Tn7-Based device for calibrated heterologous gene expression in *Pseudomonas putida*. *ACS Synth. Biol.* **4**, 1341–1351 (2015).
61. Molina-Santiago, C. et al. *Pseudomonas putida* as a platform for the synthesis of aromatic compounds. *Microbiology* **162**, 1535–1543 (2016).
62. Nikel, P. I., Pérez-Pantoja, D. & de Lorenzo, V. Pyridine nucleotide transhydrogenases enable redox balance of *Pseudomonas putida* during biodegradation of aromatic compounds. *Environ. Microbiol.* **18**, 3565–3582 (2016).

63. Jha, R. K. et al. A protocatechuate biosensor for *Pseudomonas putida* KT2440 via promoter and protein evolution. *Metab. Eng. Commun.* **6**, 33–38 (2018).
64. Machado, L. F. M., Currin, A. & Dixon, N. Directed evolution of the PcaV allosteric transcription factor to generate a biosensor for aromatic aldehydes. *J. Biol. Eng.* **13**, 91 (2019).
65. Upadhyaya, B. P., DeVaux, L. C. & Christopher, L. P. Metabolic engineering as a tool for enhanced lactic acid production. *Trends Biotechnol.* **32**, 637–644 (2014).
66. Son, J. et al. Microbial cell factories for the production of three-carbon backbone organic acids from agro-industrial wastes. *Biores. Technol.* **349**, 126797 (2022).
67. Bernal, P., Allsopp, L. P., Filloux, A. & Llamas, M. A. The *Pseudomonas putida* T6SS is a plant warden against phytopathogens. *ISME J.* **11**, 972–987 (2017).
68. Futai, M. Membrane D-lactate dehydrogenase from *Escherichia coli*. Purification and properties. *Biochemistry* **12**, 2468–2474 (1973).
69. Mutalik, V. K. et al. Precise and reliable gene expression via standard transcription and translation initiation elements. *Nat. Methods* **10**, 354–360 (2013).
70. Bird, J. E., Marles-Wright, J. & Giachino, A. A user's guide to Golden Gate cloning methods and standards. *ACS Synth. Biol.* **11**, 3551–3563 (2022).
71. Bujdoš, D. et al. Engineering of *Pseudomonas putida* for accelerated co-utilization of glucose and cellobiose yields aerobic overproduction of pyruvate explained by an upgraded metabolic model. *Metab. Eng.* **75**, 29–46 (2023).
72. Palm, G. J. et al. Structure of the plastic-degrading *Ideonella sakaiensis* MHETase bound to a substrate. *Nat. Commun.* **10**, 1717 (2019).
73. Yoshida, S. et al. A bacterium that degrades and assimilates poly(ethylene terephthalate). *Science* **351**, 1196–1199 (2016).
74. Zurier, H. S. & Goddard, J. M. A high-throughput expression and screening platform for applications-driven PETase engineering. *Biotechnol. Bioeng.* **120**, 1000–1014 (2023).
75. Liu, K. et al. A dual fluorescence assay enables high-throughput screening for poly(ethylene terephthalate) hydrolases. *ChemSusChem* **16**, e202202019 (2023).
76. Heyde, S. A. H., Arnling Bååth, J., Westh, P., Nørholm, M. H. H. & Jensen, K. Surface display as a functional screening platform for detecting enzymes active on PET. *Microb. Cell Fact.* **20**, 93 (2021).
77. Lu, H. et al. Machine learning-aided engineering of hydrolases for PET depolymerization. *Nature* **604**, 662–667 (2022).
78. Kenny, S. T. et al. Up-cycling of PET (polyethylene terephthalate) to the biodegradable plastic PHA (polyhydroxyalkanoate). *Environ. Sci. Technol.* **42**, 7696–7701 (2008).
79. Narancic, T. et al. Genome analysis of the metabolically versatile *Pseudomonas umsongensis* GO16: the genetic basis for PET monomer upcycling into polyhydroxyalkanoates. *Microb. Biotechnol.* **14**, 2463–2480 (2021).
80. Jiménez, J. I., Miñambres, B., García, J. L. & Díaz, E. Genomic analysis of the aromatic catabolic pathways from *Pseudomonas putida* KT2440. *Environ. Microbiol.* **4**, 824–841 (2002).
81. Mohamed, E. T. et al. Adaptive laboratory evolution of *Pseudomonas putida* KT2440 improves *p*-coumaric and ferulic acid catabolism and tolerance. *Metab. Eng. Commun.* **11**, e00143 (2020).
82. Kasai, D., Kitajima, M., Fukuda, M. & Masai, E. Transcriptional regulation of the terephthalate catabolism operon in *Comamonas* sp. strain E6. *Appl. Environ. Microbiol.* **76**, 6047–6055 (2010).
83. Cetnar, D. P. & Salis, H. M. Systematic quantification of sequence and structural determinants controlling mRNA stability in bacterial operons. *ACS Synth. Biol.* **10**, 318–332 (2021).
84. Pardo, I. et al. Gene amplification, laboratory evolution, and biosensor screening reveal Muck as a terephthalic acid transporter in *Acinetobacter baylyi* ADP1. *Metab. Eng.* **62**, 260–274 (2020).
85. Son, H. F. et al. Rational protein engineering of thermo-stable PETase from *Ideonella sakaiensis* for highly efficient PET degradation. *ACS Catal.* **9**, 3519–3526 (2019).
86. Hong, H. et al. Discovery and rational engineering of PET hydrolase with both mesophilic and thermophilic PET hydrolase properties. *Nat. Commun.* **14**, 4556 (2023).
87. Werner, A. Z. et al. Tandem chemical deconstruction and biological upcycling of poly(ethylene terephthalate) to β -keto adipic acid by *Pseudomonas putida* KT2440. *Metab. Eng.* **67**, 250–261 (2021).
88. Mückschel, B. et al. Ethylene glycol metabolism by *Pseudomonas putida*. *Appl. Environ. Microbiol.* **78**, 8531–8539 (2012).
89. Li, W. J. et al. Laboratory evolution reveals the metabolic and regulatory basis of ethylene glycol metabolism by *Pseudomonas putida* KT2440. *Environ. Microbiol.* **21**, 3669–3682 (2019).
90. Franden, M. A. et al. Engineering *Pseudomonas putida* KT2440 for efficient ethylene glycol utilization. *Metab. Eng.* **48**, 197–207 (2018).
91. Sulaiman, S. et al. Isolation of a novel cutinase homolog with polyethylene terephthalate-degrading activity from leaf-branch compost by using a metagenomic approach. *Appl. Environ. Microbiol.* **78**, 1556–1562 (2012).
92. Hernandez-Valdes, J. A. et al. Enhancement of amino acid production and secretion by *Lactococcus lactis* using a droplet-based biosensing and selection system. *Metab. Eng. Commun.* **11**, e00133 (2020).
93. Bowman, E. K. et al. Sorting for secreted molecule production using a biosensor-in-microdroplet approach. *Proc. Natl. Acad. Sci. USA* **118**, e2106818118 (2021).
94. Bertels, F., Merker, H. & Kost, C. Design and characterization of auxotrophy-based amino acid biosensors. *PLoS One* **7**, e41349 (2012).
95. Pflieger, B. F., Pitera, D. J., Newman, J. D., Martin, V. J. J. & Keasling, J. D. Microbial sensors for small molecules: development of a mevalonate biosensor. *Metab. Eng.* **9**, 30–38 (2007).
96. Dvořák, P., Nikel, P. I., Damborský, J. & de Lorenzo, V. *Bioremediation 3.0*: engineering pollutant-removing bacteria in the times of systemic biology. *Biotechnol. Adv.* **35**, 845–866 (2017).
97. Khan, M. F. & Murphy, C. D. Bacterial degradation of the antidepressant drug fluoxetine produces trifluoroacetic acid and fluoride ion. *Appl. Microbiol. Biotechnol.* **105**, 9359–9369 (2021).
98. Holert, J. et al. Bacteria use a catabolic patchwork pathway of apparently recent origin for degradation of the synthetic buffer compound TRIS. *ISME J.* **18**, wrad023 (2024).
99. Baba, T. et al. Construction of *Escherichia coli* K-12 in-frame, single-gene knockout mutants: the Keio collection. *Mol. Syst. Biol.* **2**, 2006.0008 (2006).
100. Banerjee, D. et al. Genome-scale metabolic rewiring improves titers rates and yields of the non-native product indigoidine at scale. *Nat. Commun.* **11**, 5385 (2020).
101. O'Brien, E. J., Lerman, J. A., Chang, R. L., Hyduke, D. R. & Palsson, B. Ø. Genome-scale models of metabolism and gene expression extend and refine growth phenotype prediction. *Mol. Syst. Biol.* **9**, 693 (2013).
102. Kim, P. J. et al. Metabolite essentiality elucidates robustness of *Escherichia coli* metabolism. *Proc. Natl. Acad. Sci. USA* **104**, 13638–13642 (2007).
103. Paul, C. et al. Enzyme engineering for biocatalysis. *Mol. Catal.* **555**, 113874 (2024).
104. Mazurenko, S., Prokop, Z. & Damborsky, J. Machine learning in enzyme engineering. *ACS Catal.* **10**, 1210–1223 (2020).
105. Guan, A., He, Z., Wang, X., Jia, Z. J. & Qin, J. Engineering the next-generation synthetic cell factory driven by protein engineering. *Biotechnol. Adv.* **73**, 108366 (2024).
106. Cai, J. et al. Review of physicochemical properties and analytical characterization of lignocellulosic biomass. *Renew. Sust. Energy Rev.* **76**, 309–322 (2017).

107. Kang, M. K., Yoon, S. H., Kwon, M. & Kim, S. W. Microbial cell factories for bio-based isoprenoid production to replace fossil resources. *Curr. Opin. Syst. Biol.* **37**, 100502 (2024).
108. Moreno-Bondi, M. C. et al. From detection to remediation: analytical science at the forefront of environmental research. *Anal. Chem.* **94**, 14811–14814 (2022).
109. Calero, P. & Nikel, P. I. Chasing bacterial chassis for metabolic engineering: a perspective review from classical to non-traditional microorganisms. *Microb. Biotechnol.* **12**, 98–124 (2019).
110. Gantz, M., Neun, S., Medcalf, E. J., van Vliet, L. D. & Hollfelder, F. Ultrahigh-throughput enzyme engineering and discovery in in vitro compartments. *Chem. Rev.* **123**, 5571–5611 (2023).
111. Wang, Y. et al. Directed evolution: methodologies and applications. *Chem. Rev.* **121**, 12384–12444 (2021).
112. Xu, L. et al. Mapping enzyme catalysis with metabolic biosensing. *Nat. Commun.* **12**, 6803 (2021).
113. Hartmans, S., Smits, J. P., van der Werf, M. J., Volkering, F. & de Bont, J. A. Metabolism of styrene oxide and 2-phenylethanol in the styrene-degrading *Xanthobacter* strain 124X. *Appl. Environ. Microbiol.* **55**, 2850–2855 (1989).
114. Nikel, P. I., Pettinari, M. J., Ramirez, M. C., Galvagno, M. A. & Méndez, B. S. *Escherichia coli arcA* mutants: metabolic profile characterization of microaerobic cultures using glycerol as a carbon source. *J. Mol. Microbiol. Biotechnol.* **15**, 48–54 (2008).
115. Clark, D. J. & Maaløe, O. DNA replication and the division cycle in *Escherichia coli*. *J. Mol. Biol.* **23**, 99–112 (1967).
116. Wirth, N. T., Funk, J., Donati, S. & Nikel, P. I. *QurvE*: user-friendly software for the analysis of biological growth and fluorescence data. *Nat. Protoc.* **18**, 2401–2403 (2023).
117. Kozaeva, E. et al. Model-guided dynamic control of essential metabolic nodes boosts acetyl-coenzyme A-dependent bioproduction in rewired *Pseudomonas putida*. *Metab. Eng.* **67**, 373–386 (2021).
118. Fernández-Cabezón, L., Cros, A. & Nikel, P. I. Spatiotemporal manipulation of the mismatch repair system of *Pseudomonas putida* accelerates phenotype emergence. *ACS Synth. Biol.* **10**, 1214–1226 (2021).
119. Blin, K., Pedersen, L. E., Weber, T. & Lee, S. Y. CRISpy-web: an online resource to design sgRNAs for CRISPR applications. *Synth. Syst. Biotechnol.* **1**, 118–121 (2016).
120. Stukenberg, D. et al. The Marburg Collection: a Golden Gate DNA assembly framework for synthetic biology applications in *Vibrio natriegens*. *ACS Synth. Biol.* **10**, 1904–1919 (2021).
121. Wirth, N. T. et al. A synthetic C2 auxotroph of *Pseudomonas putida* for evolutionary engineering of alternative sugar catabolic routes. *Metab. Eng.* **74**, 83–97 (2022).
122. Choi, K. H. et al. A Tn7-based broad-range bacterial cloning and expression system. *Nat. Methods* **2**, 443–448 (2005).
123. Arnling Bååth, J., Jensen, K., Borch, K., Westh, P. & Kari, J. Sabatier principle for rationalizing enzymatic hydrolysis of a synthetic polyester. *JACS Au* **2**, 1223–1231 (2022).
124. Sambrook, J. & Russell, D. W. *Molecular Cloning: A Laboratory Manual*, Edn. 3rd. (Cold Spring Harbor Laboratory, Cold Spring Harbor, 2001).
125. Erickson, E. et al. Comparative performance of PETase as a function of reaction conditions, substrate properties, and product accumulation. *ChemSusChem* **15**, e202101932 (2022).
- Foundation (NNF10CC1016517, and NNF18CC0033664, and NNF23OC0083631) to P.I.N. is gratefully acknowledged. The responsibility of this article lies with the authors; the NNF is not responsible for any use that may be made of the information contained therein.

Author contributions

J.M.H.S.: Investigation (genome engineering of *Pseudomonas putida*, growth assays, adaptive laboratory evolution, genome sequencing and analysis), Data curation, Methodology, Validation, Visualization, Writing—original draft; A.B.: Investigation (genome engineering of *Pseudomonas putida*, growth assays), Data curation; M.V.G.A.V.: Investigation (genome engineering of *Escherichia coli*, *ldhA* library cloning), Data curation; D.F.: Investigation (genome engineering of *Pseudomonas putida* for PET degradation, co-culture experiments), Data curation, Methodology; J.A.B.: Investigation (enzymatic PET degradation), Data curation, Methodology; P.W.: Resources, Supervision; K.J.: Resources, Supervision; L.N.G.: Methodology, Supervision, Resources; D.C.V.: Conceptualization, Investigation, Data curation, Methodology, Validation, Visualization, Writing – original draft, review & editing; P.I.N.: Methodology, Validation, Visualization, Resources, Data curation, Funding acquisition, Supervision, Project administration, Writing—review & editing.

Competing interests

The authors declare no competing interests.

Additional information

Supplementary information The online version contains supplementary material available at <https://doi.org/10.1038/s41467-024-52755-y>.

Correspondence and requests for materials should be addressed to Daniel C. Volke or Pablo I. Nikel.

Peer review information *Nature Communications* thanks the anonymous reviewers for their contribution to the peer review of this work. A peer review file is available.

Reprints and permissions information is available at <http://www.nature.com/reprints>

Publisher's note Springer Nature remains neutral with regard to jurisdictional claims in published maps and institutional affiliations.

Open Access This article is licensed under a Creative Commons Attribution-NonCommercial-NoDerivatives 4.0 International License, which permits any non-commercial use, sharing, distribution and reproduction in any medium or format, as long as you give appropriate credit to the original author(s) and the source, provide a link to the Creative Commons licence, and indicate if you modified the licensed material. You do not have permission under this licence to share adapted material derived from this article or parts of it. The images or other third party material in this article are included in the article's Creative Commons licence, unless indicated otherwise in a credit line to the material. If material is not included in the article's Creative Commons licence and your intended use is not permitted by statutory regulation or exceeds the permitted use, you will need to obtain permission directly from the copyright holder. To view a copy of this licence, visit <http://creativecommons.org/licenses/by-nc-nd/4.0/>.

© The Author(s) 2024

Acknowledgements

We thank Dr. José I. Jiménez-Zarco (Imperial College London, UK) for sharing research materials. The financial support from The Novo Nordisk